Table 3. Multivariate analysis of variables relevant to survival, local tumor progression, and distant recurrence

Variable	Multivariate analysis Hazard ratio (95% CI)	*P* value
Survival		
Age (per year)	1.03 (1.02–1.04)	<0.0001
Anti-HCV-positive	1.34 (1.03–1.76)	0.03
Child-Pugh class		
A	1	
B or C	2.08 (1.69–2.56)	<0.0001
Tumor size (cm)		
≤2.0	1	
2.1–3.0	1.40 (1.10–1.80)	0.007
3.1–5.0	1.80 (1.37–2.38)	<0.0001
>5.0	1.50 (0.90–2.49)	0.12
Tumor number		
Solitary	1	
2–3	1.28 (1.04–1.59)	0.02
≥4	1.58 (1.13–2.21)	0.008
Serum DCP (mAU/ml)		
≤100	1	
101–400	1.22 (0.88–1.69)	0.24
>400	1.66 (1.14–2.42)	0.008
Serum AFP-L3 (%)		
≤15	1	
>15	1.45 (1.11–1.91)	0.008
Local tumor progression		
Serum DCP (mAU/ml)		
≤100	1	
101–400	2.51 (1.02–6.20)	0.05
>400	6.52 (2.63–16.1)	<0.0001
Distant recurrence		
Anti-HCV-positive	1.44 (1.19–1.75)	0.0002
Child-Pugh class		
A	1	
B or C	1.23 (1.03–1.45)	0.02
Platelet count (/l)		
$>10^{11}$	1	
$\leq 10^{11}$	1.36 (1.12–1.64)	0.002
Tumor size (cm)		
≤2.0	1	
2.1–3.0	1.30 (1.10–1.55)	0.003
3.1–5.0	1.29 (1.05–1.60)	0.02
>5.0	1.25 (0.75–2.08)	0.4
Tumor number		
Solitary	1	
2–3	1.36 (1.16–1.59)	0.0002
≥4	2.02 (1.53–2.66)	<0.0001
Serum AFP (ng/dl)		
≤100	1	
101–400	1.15 (0.92–1.44)	0.22
>400	1.36 (1.03–1.81)	0.03
Serum DCP (mAU/ml)		
≤100	1	
101–400	1.19 (0.92–1.54)	0.19
>400	1.72 (1.22–2.42)	0.002

AFP, α-fetoprotein; CI, confidence interval; DCP, des-γ-carboxy-prothrombin; HCV, hepatitis C virus.

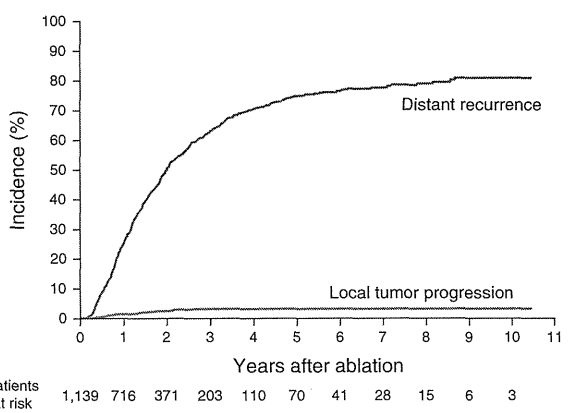

Figure 3. Local tumor progression and distant recurrence in patients who underwent radiofrequency ablation.

This study shows that RFA could achieve long-term survival for as long as 10 years. Sixteen patients treated by RFA survived for >10 years. The variables relevant to survival were similar to those found in previous studies on ethanol injection (26,27), RFA, hepatic resection (28), and transarterial chemoembolization (29). Both liver function and tumor-related factors were associated with survival. In addition, age and anti-HCV were relevant to survival in this study. Age was among the prognostic factors, probably because 23.0% of the patients were >75 years old, which resulted in a higher percentage (18.5%) of liver-unrelated deaths in this study compared with others. Anti-HCV was among the prognostic factors, probably because anti-HCV-positive patients developed distant recurrence more frequently.

HCC frequently recurred after RFA; most recurrences were, however, not local tumor progression but distant recurrence. Frequent recurrence is not specific to RFA. After hepatic resection, the

Table 4. Complications in 2,982 treatments of radiofrequency ablation for hepatocellular carcinoma

Complication	No. of complications
Neoplastic seeding	24
Liver abscess	6
Hemoperitoneum	12
Hemothorax	5
Symptomatic pleural effusion	1
Massive hepatic infarction	6
Gastrointestinal perforation or penetration	5
Hemobilia	2
Skin burn	1
Pneumothorax	3
Gallbladder injury	1
Cerebral infarction	1

tumor recurrence rate exceeds 70% at 5 years (30,31). In this study, periodic follow-up detected most recurrences at limited stage. RFA was performed again for first recurrence in almost 90% of cases, although multimodal treatments were used in a long-term follow-up. On the other hand, repeat resection rate for first recurrence has been reported to range from 10.4 to 30.6% (31,32). Because RFA is less invasive than hepatic resection, iterative RFA can be performed for recurrence more easily.

Local tumor progression was found less frequently in this study than in other studies, having been reported to be around 10% at 3 years following RFA (13,14). Furthermore, different from the findings in previous reports (33,34), tumor size was not related to local tumor progression in this study. These differences are probably because we repeated RFA until we considered we had ablated not only the tumor itself but also some of the liver tissue surrounding it. Furthermore, to avoid local tumor progression, we were more cautious in the treatment of larger tumors when deciding whether sufficient ablation had been performed. Only serum DCP level was significantly related to local tumor progression in this study. Elevated serum DCP level may be related to the malignant potential of HCC such as the development of portal venous invasion (35).

The frequency of distant recurrence in this study was similar to that reported in other studies (13). Among the variables significantly related to distant recurrence, tumor size, tumor number, serum AFP level, and serum DCP level were probably related to micrometastasis, which had not been detected by imaging modalities before the treatment, while anti-HCV, Child-Pugh class, and platelet count were related to metachronous multicentric carcinogenesis, which developed based on underlying chronic liver disease.

From the viewpoint of survival and distant recurrence, patients with 2.1–5.0 cm tumors had significantly worse outcomes than those with ≤2.0 cm tumors while those with tumors >5.0 cm did not have worse rates than those with tumors ≤2 cm. This is probably because the number of patients with tumors >5.0 cm ($n=35$) were not large enough for the difference to be statistically significant. Another possibility is selection bias. It is possible that patient with tumors >5.0 cm who underwent RFA had more favorable conditions for survival and distant recurrence except tumor size than those with 2.1–5.0 cm tumors.

In this study, 324 of the 1,170 patients were treated with combination of TACE and RFA at the initial treatment. Thus, we evaluated the combination as a possible variable that influences survival or recurrence. Univariate analysis demonstrated that the combined therapy was significantly correlated to overall survival, whereas multivariate analysis did not show the relationship. TACE was generally combined with RFA in patients with either ≥4 tumors or those with even one tumor >3.0 cm in diameter. This is why the correlation was significant in univariate analysis, while it was not in multivariable model in which the effect of other risk factors, such as tumor number and tumor size were adjusted. The combination of TACE and RFA was not significantly related to either local tumor progression or distant recurrence.

RFA was a safe procedure. Although many patients treated by RFA in this study were at high risk for surgical treatment because of advanced cirrhosis or other comorbidities, complications occurred in only 2.2% of the treatments. Other investigators have also reported low complication rates of 0–6.1% (11,13–16). For hepatic resection, morbidity rates of 38–47% have been reported even in recent studies (36–38).

To date, percutaneous ethanol injection has been considered the standard in ablation (5). However, randomized controlled trials have demonstrated the superiority of RFA (6–9), with RFA now largely replacing ethanol injection. We have also shifted from ethanol injection to RFA (10). At our department, RFA is currently the first option and ethanol injection is performed only on patients on whom RFA cannot be performed safely because of either enterobiliary reflux, adhesion between the tumor and the gastrointestinal tract, or other reasons.

Surgical resection has been considered the treatment of choice for HCC. Our first option for resectable HCC was also surgery. However, most patients who came to our department visited us because they did not want surgical resection. Thus, many patients in this study underwent RFA not because of unresectable tumor but because of refusal of surgery. Those who preferred surgery would have directly gone to the surgical department that has extensive experience in hepatic resection (38).

It is not easy to compare outcomes between RFA and surgical resection; the indications are different between the two treatments. Furthermore, indications for each treatment are different from institution to institution. Thus, a case adjudged to be treatable by RFA or surgical resection at an institution may not be given the same treatment at another. The best known indication criteria for surgical resection may be those proposed in the Barcelona Clinic Liver Cancer (BCLC) protocol (5), which states that surgical resection should be restricted to patients with performance status 0, Child-Pugh class A, single HCC, normal portal pressure, and normal serum bilirubin level. In patients satisfying those criteria, the 5-year survival rate is expected to be >70% (30). In this study, 237

© 2012 by the American College of Gastroenterology

(20.3%) of 1,170 patients satisfied those criteria and were thus considered good candidates for surgical resection; their 5-year survival rate was 75.9%, which appears satisfactory when compared with outcomes following surgical resection. Furthermore, in all 1,170 primary HCC patients treated by RFA, 5- and 10-year survival rates were 60.2% and 27.3%, respectively. In patients treated by surgical resection, 5- and 10-year survival rates were 34.4–70.0% and 10.5–52.0%, respectively (32,39–45). Although this is an observational study with no control, survivals following RFA appear comparable to those reported following surgical resection.

Two recent randomized controlled trials showed no significant difference in survival between RFA and surgical resection (46,47). Several nonrandomized controlled trials reported that RFA had similar overall survival rates to resection (48–50), while others found resection to be associated with higher survival rates (51–53). Further studies are necessary to resolve comparison of RFA with resection.

We have made strenuous efforts to standardize the RFA procedure. Although many physicians have participated in RFA at our institution, the procedure was invariably performed according to the institutional protocol and in the presence of experienced physicians. Video recording was also used to monitor the procedure. Additionally, preoperative planning and postoperative evaluation of technique effectiveness were also carried out by at least three physicians. We also believe that not only proficient practice of RFA but also detailed preoperative planning, cautious postoperative evaluation of therapeutic effect, and careful follow-up are vital to achieve satisfactory outcomes.

Source population in this study may represent selection bias, as we performed RFA on most patients who were hospitalized at our department; however, many patients with unfavorable tumor conditions for RFA might not have been referred to us. Therefore, caution is required when extrapolating our findings to the general population of HCC patients.

A second limitation is that study population cannot be clearly defined. This study was based on daily clinical practice over a 10-year period. Indication criteria of RFA have changed over time, mainly because another percutaneous ablation, that is, ethanol injection has also been performed. Furthermore, various treatments besides percutaneous ablation were available for HCC, such as surgical resection and transarterial chemoembolization, with frequently overlapping indications.

One further limitation is the fact that this was a single-center study; these results might not be reproducible consistently in other settings. To extrapolate the findings in this study to patients at other institutions, careful consideration should be given to differences in the indications, methods, expertise, performance of available ultrasound and CT equipment, and others. Treatment outcome may be influenced by the physicians' expertise and the institution's volume of care. We started ethanol injection in 1985 and microwave ablation in 1995, that is, before the introduction of RFA. Recently, we have performed over 900 RFA treatments per year, which may represent a far greater number of treatments than those in most other institutions. We would not recommend any change in daily clinical practice solely on the strength of our study findings.

In conclusion, our 10-year clinical experience shows that RFA could be locally curative, resulting in survival for as long as 10 years, and was a safe procedure. RFA might be a first-line treatment for selected patients with early-stage HCC.

CONFLICT OF INTEREST

Guarantor of the article: Shuichiro Shiina, MD, PhD.

Specific author contributions: Study concept and design, analysis and interpretation of data, and drafting of the manuscript: Shuichiro Shiina; analysis and interpretation of data and statistical analysis: Ryosuke Tateishi; study execution and data acquisition: Toru Arano, Koji Uchino, Kenichiro Enooku, Hayato Nakagawa, Yoshinari Asaoka, Takahisa Sato, Ryota Masuzaki, Yuji Kondo, and Tadashi Goto; revised the article critically for important intellectual content: Haruhiko Yoshida; Masao Omata, and Kazuhiko Koike. All authors have read and approved the submitted manuscript.

Financial support: This study was partly supported by Health Sciences Research Grants of The Ministry of Health, Labor and Welfare of Japan (Research on Hepatitis).

Potential competing interests: None.

Study Highlights

WHAT IS CURRENT KNOWLEDGE

- ✓ Radiofrequency ablation (RFA) has been widely performed for hepatocellular carcinoma (HCC).
- ✓ RFA has a more reliable local antitumor effect and higher survival than ethanol injection.
- ✓ There has been no report on 10-year outcome of RFA.

WHAT IS NEW HERE

- ✓ Five- and 10-year survival rates in 1,170 patients with primary hepatocellular carcinoma (HCC) were 60.2 and 27.3%, respectively.
- ✓ Age, antibody to hepatitis C virus, Child-Pugh class, tumor size, tumor number, serum des-γ-carboxy-prothrombin level, and serum lectin-reactive α-fetoprotein level were significantly related to survival.
- ✓ Five- and 10-year local tumor progression rates were both 3.2%. Five- and 10-year distant recurrence rates were 74.8 and 80.8%, respectively.

REFERENCES

1. Parkin DM, Bray F, Ferlay J *et al.* Estimating the world cancer burden: Globocan 2000. Int J Cancer 2001;94:153–6.
2. Borie F, Bouvier AM, Herrero A *et al.* Treatment and prognosis of hepatocellular carcinoma: a population based study in France. J Surg Oncol 2008;98:505–9.
3. Ryder SD. Guidelines for the diagnosis and treatment of hepatocellular carcinoma (HCC) in adults. Gut 2003;52 (Suppl 3): iii1–8.
4. Llovet JM, Burroughs A, Bruix J. Hepatocellular carcinoma. Lancet 2003;362:1907–17.
5. Bruix J, Sherman M. Management of hepatocellular carcinoma. Hepatology 2005;42:1208–36.
6. Shiina S, Teratani T, Obi S *et al.* A randomized controlled trial of radiofrequency ablation with ethanol injection for small hepatocellular carcinoma. Gastroenterology 2005;129:122–30.
7. Lin SM, Lin CJ, Lin CC *et al.* Radiofrequency ablation improves prognosis compared with ethanol injection for hepatocellular carcinoma ≤4 cm. Gastroenterology 2004;127:1714–23.

8. Lin SM, Lin CJ, Lin CC *et al.* Randomised controlled trial comparing percutaneous radiofrequency thermal ablation, percutaneous ethanol injection, and percutaneous acetic acid injection to treat hepatocellular carcinoma of 3 cm or less. Gut 2005;54:1151–6.
9. Lencioni RA, Allgaier HP, Cioni D *et al.* Small hepatocellular carcinoma in cirrhosis: randomized comparison of radio-frequency thermal ablation versus percutaneous ethanol injection. Radiology 2003;228:235–40.
10. Shiina S, Teratani T, Obi S *et al.* Nonsurgical treatment of hepatocellular carcinoma: from percutaneous ethanol injection therapy and percutaneous microwave coagulation therapy to radiofrequency ablation. Oncology 2002;62 (Suppl 1): 64–8.
11. N'Kontchou G, Mahamoudi A, Aout M *et al.* Radiofrequency ablation of hepatocellular carcinoma: long-term results and prognostic factors in 235 Western patients with cirrhosis. Hepatology 2009;50:1475–83.
12. Tateishi R, Shiina S, Teratani T *et al.* Percutaneous radiofrequency ablation for hepatocellular carcinoma. An analysis of 1000 cases. Cancer 2005;103:1201–9.
13. Lencioni R, Cioni D, Crocetti L *et al.* Early-stage hepatocellular carcinoma in patients with cirrhosis: long-term results of percutaneous image-guided radiofrequency ablation. Radiology 2005;234:961–7.
14. Choi D, Lim HK, Rhim H *et al.* Percutaneous radiofrequency ablation for early-stage hepatocellular carcinoma as a first-line treatment: long-term results and prognostic factors in a large single-institution series. Eur Radiol 2007;17:684–92.
15. Livraghi T, Meloni F, Di Stasi M *et al.* Sustained complete response and complications rates after radiofrequency ablation of very early hepatocellular carcinoma in cirrhosis: is resection still the treatment of choice? Hepatology 2008;47:82–9.
16. Buscarini L, Buscarini E, Di Stasi M *et al.* Percutaneous radiofrequency ablation of small hepatocellular carcinoma: long-term results. Eur Radiol 2001;11:914–21.
17. Raut CP, Izzo F, Marra P *et al.* Significant long-term survival after radiofrequency ablation of unresectable hepatocellular carcinoma in patients with cirrhosis. Ann Surg Oncol 2005;12:616–28.
18. Teratani T, Yoshida H, Shiina S *et al.* Radiofrequency ablation for hepatocellular carcinoma in so-called high-risk locations. Hepatology 2006;43:1101–8.
19. Araki T, Itai Y, Furui S *et al.* Dynamic CT densitometry of hepatic tumors. AJR Am J Roentgenol 1980;135:1037–43.
20. Kondo Y, Yoshida H, Tateishi R *et al.* Percutaneous radiofrequency ablation of liver cancer in the hepatic dome using the intrapleural fluid infusion technique. Br J Surg 2008;95:996–1004.
21. Kondo Y, Yoshida H, Shiina S *et al.* Artificial ascites technique for percutaneous radiofrequency ablation of liver cancer adjacent to the gastrointestinal tract. Br J Surg 2006;93:1277–82.
22. Goldberg SN, Grassi CJ, Cardella JF *et al.* Image-guided tumor ablation: standardization of terminology and reporting criteria. Radiology 2005;235:728–39.
23. Gaynor JJ, Feuer EJ, Tan CC *et al.* On the use of cause-specific failure and conditional failure probabilities: examples from clinical oncology data. J Am Stat Assoc 1993;88:400–9.
24. Sacks D, McClenny TE, Cardella JF *et al.* Society of interventional radiology clinical practice guidelines. J Vasc Interv Radiol 2003;14:S199–202.
25. Sala M, Llovet JM, Vilana R *et al.* Initial response to percutaneous ablation predicts survival in patients with hepatocellular carcinoma. Hepatology 2004;40:1352–60.
26. Lencioni R, Bartolozzi C, Caramella D *et al.* Treatment of small hepatocellular carcinoma with percutaneous ethanol injection. Analysis of prognostic factors in 105 Western patients. Cancer 1995;76:1737–46.
27. Castellano L, Calandra M, Del Vecchio Blanco C *et al.* Predictive factors of survival and intrahepatic recurrence of hepatocellular carcinoma in cirrhosis after percutaneous ethanol injection: analysis of 71 patients. J Hepatol 1997;27:862–70.
28. Franco D, Capussotti L, Smadja C *et al.* Resection of hepatocellular carcinomas. Results in 72 European patients with cirrhosis. Gastroenterology 1990;98:733–8.
29. Takayasu K, Arii S, Ikai I *et al.* Prospective cohort study of transarterial chemoembolization for unresectable hepatocellular carcinoma in 8510 patients. Gastroenterology 2006;131:461–9.
30. Llovet JM, Fuster J, Bruix J. Intention-to-treat analysis of surgical treatment for early hepatocellular carcinoma: resection versus transplantation. Hepatology 1999;30:1434–40.
31. Minagawa M, Makuuchi M, Takayama T *et al.* Selection criteria for repeat hepatectomy in patients with recurrent hepatocellular carcinoma. Ann Surg 2003;238:703–10.
32. Poon RT, Fan ST, Lo CM *et al.* Long-term survival and pattern of recurrence after resection of small hepatocellular carcinoma in patients with preserved liver function: implications for a strategy of salvage transplantation. Ann Surg 2002;235:373–82.
33. Ishii H, Okada S, Nose H *et al.* Local recurrence of hepatocellular carcinoma after percutaneous ethanol injection. Cancer 1996;77:1792–6.
34. Mulier S, Ni Y, Jamart J *et al.* Local recurrence after hepatic radiofrequency coagulation: multivariate meta-analysis and review of contributing factors. Ann Surg 2005;242:158–71.
35. Koike Y, Shiratori Y, Sato S *et al.* Des-gamma-carboxy prothrombin as a useful predisposing factor for the development of portal venous invasion in patients with hepatocellular carcinoma: a prospective analysis of 227 patients. Cancer 2001;91:561–9.
36. Capussotti L, Muratore A, Amisano M *et al.* Liver resection for hepatocellular carcinoma on cirrhosis: analysis of mortality, morbidity and survival--a European single center experience. Eur J Surg Oncol 2005;31:986–93.
37. Taketomi A, Kitagawa D, Itoh S *et al.* Trends in morbidity and mortality after hepatic resection for hepatocellular carcinoma: an institute's experience with 625 patients. J Am Coll Surg 2007;204:580–7.
38. Imamura H, Seyama Y, Kokudo N *et al.* One thousand fifty-six hepatectomies without mortality in 8 years. Arch Surg 2003;138:1198–206; discussion 206.
39. Park YK, Kim BW, Wang HJ *et al.* Hepatic resection for hepatocellular carcinoma meeting Milan criteria in Child-Turcotte-Pugh class a patients with cirrhosis. Transplant Proc 2009;41:1691–7.
40. Wang CC, Iyer SG, Low JK *et al.* Perioperative factors affecting long-term outcomes of 473 consecutive patients undergoing hepatectomy for hepatocellular carcinoma. Ann Surg Oncol 2009;16:1832–42.
41. Kamiyama T, Nakanishi K, Yokoo H *et al.* Recurrence patterns after hepatectomy of hepatocellular carcinoma: implication of Milan criteria utilization. Ann Surg Oncol 2009;16:1560–71.
42. Yamamoto J, Kosuge T, Saiura A *et al.* Effectiveness of hepatic resection for early-stage hepatocellular carcinoma in cirrhotic patients: subgroup analysis according to Milan criteria. Jpn J Clin Oncol 2007;37:287–95.
43. Nuzzo G, Giuliante F, Gauzolino R *et al.* Liver resections for hepatocellular carcinoma in chronic liver disease: experience in an Italian centre. Eur J Surg Oncol 2007;33:1014–8.
44. Hanazaki K, Kajikawa S, Shimozawa N *et al.* Survival and recurrence after hepatic resection of 386 consecutive patients with hepatocellular carcinoma. J Am Coll Surg 2000;191:381–8.
45. Shimada K, Sano T, Sakamoto Y *et al.* A long-term follow-up and management study of hepatocellular carcinoma patients surviving for 10 years or longer after curative hepatectomy. Cancer 2005;104:1939–47.
46. Chen MS, Li JQ, Zheng Y *et al.* A prospective randomized trial comparing percutaneous local ablative therapy and partial hepatectomy for small hepatocellular carcinoma. Ann Surg 2006;243:321–8.
47. Lu MD, Kuang M, Liang LJ *et al.* [Surgical resection versus percutaneous thermal ablation for early-stage hepatocellular carcinoma: a randomized clinical trial]. Zhonghua Yi Xue Za Zhi 2006;86:801–5.
48. Hong SN, Lee SY, Choi MS *et al.* Comparing the outcomes of radiofrequency ablation and surgery in patients with a single small hepatocellular carcinoma and well-preserved hepatic function. J Clin Gastroenterol 2005;39:247–52.
49. Yamagiwa K, Shiraki K, Yamakado K *et al.* Survival rates according to the Cancer of the Liver Italian Program scores of 345 hepatocellular carcinoma patients after multimodality treatments during a 10-year period in a retrospective study. J Gastroenterol Hepatol 2008;23:482–90.
50. Yamakado K, Nakatsuka A, Takaki H *et al.* Early-stage hepatocellular carcinoma: radiofrequency ablation combined with chemoembolization versus hepatectomy. Radiology 2008;247:260–6.
51. Vivarelli M, Guglielmi A, Ruzzenente A *et al.* Surgical resection versus percutaneous radiofrequency ablation in the treatment of hepatocellular carcinoma on cirrhotic liver. Ann Surg 2004;240:102–7.
52. Guglielmi A, Ruzzenente A, Valdegamberi A *et al.* Radiofrequency ablation versus surgical resection for the treatment of hepatocellular carcinoma in cirrhosis. J Gastrointest Surg 2008;12:192–8.
53. Abu-Hilal M, Primrose JN, Casaril A *et al.* Surgical resection versus radiofrequency ablation in the treatment of small unifocal hepatocellular carcinoma. J Gastrointest Surg 2008;12:1521–6.

SOME RIGHTS RESERVED This work is licensed under the Creative Commons Attribution-NonCommercial-Share Alike 3.0 Unported License. To view a copy of this license, visit http://creativecommons.org/licenses/by-nc-sa/3.0/

J Gastroenterol (2012) 47:71–78
DOI 10.1007/s00535-011-0462-2

ORIGINAL ARTICLE—LIVER, PANCREAS, AND BILIARY TRACT

Evaluation of molecular targeted cancer drug by changes in tumor marker doubling times

Kenichiro Enooku · Ryosuke Tateishi · Fumihiko Kanai · Yuji Kondo · Ryota Masuzaki · Tadashi Goto · Shuichiro Shiina · Haruhiko Yoshida · Masao Omata · Kazuhiko Koike

Received: 26 March 2011 / Accepted: 1 August 2011 / Published online: 21 September 2011
© Springer 2011

Abstract
Background We evaluated the usefulness of tumor marker doubling time (DT) as an efficacy indicator of a molecular targeted anticancer agent.
Methods Twenty-five patients with advanced hepatocellular carcinoma (HCC) received TSU-68, a multiple tyrosine kinase inhibitor. Exponential increase in HCC-specific tumor marker levels (alpha-fetoprotein or des-gamma-carboxyprothrombin) was seen in 15 of them prior to TSU-68 administration. The relationship between tumor marker DT and tumor volume DT was evaluated. Next, tumor marker DT in the first 8 weeks of TSU-68 administration was compared with tumor marker DT before treatment. Efficacy evaluation based on changes in tumor marker DT was compared with Response Evaluation Criteria In Solid Tumors (RECIST).
Results Tumor marker DT and tumor volume DT were almost identical ($r^2 = 0.94$, $P < 0.001$) in each patient before TSU-68 administration. Efficacy evaluation based on changes in tumor marker DT on TSU-68 administration was in accordance with RECIST in 12/15 cases. Discordance was observed in three cases, for which RECIST indicated disease progression in spite of elongated tumor marker DT. Those cases showed substantial tumor necrosis without volume shrinkage or appearance of new lesions in spite of apparent effects on target lesions.
Conclusions Serum tumor marker DT can be used to evaluate viable tumor burden irrespective of the presence of tumor necrosis which can compromise radiographic evaluation. This approach may be applicable to the evaluation of responses to chemotherapy, particularly to cytostatic agents (ClinicalTrials.gov number, NCT00784290).

Keywords Doubling time · RECIST · AFP · PIVKA-II · HCC · TSU-68

Abbreviations

AFP	Alpha-fetoprotein
CEA	Carcinoembryonic antigen
CR	Complete response
CT	Computed tomography
DCP	Des-gamma-carboxyprothrombin
DT	Doubling time
FGFR	Fibroblast growth factor receptor
HCC	Hepatocellular carcinoma
PD	Progressive disease
PDGFR	Platelet-derived growth factor receptor
PR	Partial response
PSA	Prostate-specific antigen
RECIST	Response Evaluation Criteria In Solid Tumors
SD	Stable disease
TACE	Transcatheter arterial chemoembolization
VEGFR-2	Vascular endothelial growth factor receptor-2

K. Enooku · R. Tateishi (✉) · F. Kanai · Y. Kondo · R. Masuzaki · T. Goto · S. Shiina · H. Yoshida · M. Omata · K. Koike
Department of Gastroenterology, Graduate School of Medicine, The University of Tokyo, 7-3-1 Hongo, Bunkyo-ku, Tokyo 113-8655, Japan
e-mail: tateishi-tky@umin.ac.jp

F. Kanai
Department of Gastroenterology, Chiba University Hospital, Chiba, Japan

M. Omata
Yamanashi Prefectural Central Hospital, Kofu, Japan

Introduction

Phase II trials of chemotherapeutic agents for solid tumors usually adopt an objective tumor response as the primary endpoint, the rationale being that the tumor response will be a surrogate for the effects of a particular agent on survival outcomes [1–4]. In evaluating a tumor response to a cancer drug, the Response Evaluation Criteria In Solid Tumors (RECIST) guidelines are usually adopted. However, the total tumor volume thus determined is not necessarily proportional to the number of viable tumor cells, e.g., in cases of massive tumor necrosis without tumor shrinkage [5–9].

With the progress in molecular targeted cancer drugs, concerns about the appropriate design of clinical trials of such agents have emerged [10, 11]. In contrast to conventional cytotoxic agents, molecular targeted agents often show cytostatic effects, i.e., a slowing of tumor growth. The effects of such agents upon the tumor growth rate may be better evaluated not by the changes in tumor burden but by the rate of changes for which RECIST may not be particularly suitable.

Most solid malignant tumors show an exponentially increasing volume in the natural course of their growth. The tumor volume doubling time (DT) is the parameter that defines the speed of the increase. Serum levels of several tumor markers, including prostate-specific antigen (PSA), carcinoembryonic antigen (CEA), and alpha-fetoprotein (AFP), have been reported to correlate with tumor volume in an individual patient [12–15]. The rate of changes in tumor volume may be calculated on the basis of repeated measurements of the serum tumor marker levels. The DT of serum PSA levels has also been proposed as a biological parameter that can be used to predict the prognosis of prostate cancer, and PSA determination has now become an integral part of the disease management [16–18].

The aim of the present study was to elucidate the usefulness of tumor marker DT to evaluate the efficacy of TSU-68 against hepatocellular carcinoma (HCC). TSU-68 is an orally administered, small-molecule inhibitor of multiple receptor tyrosine kinases, vascular endothelial growth factor receptor-2 (VEGFR-2), platelet-derived growth factor receptor (PDGFR), and fibroblast growth factor receptor (FGFR) [19]. As a potent antiangiogenic agent, TSU-68 is expected to be effective against HCC [20], and a phase I/II study has been recently conducted in Japan [21]. In that clinical trial, the serum levels of AFP and des-gamma-carboxyprothrombin (DCP) were also scheduled to be periodically determined. Although the effect was assessed by radiologic examinations, the effect of TSU-68 may be more accurately evaluated by changes in tumor growth speed based on specific tumor marker levels [22–26].

Methods

Clinical trial

This study was conducted according to the ethical guidelines for epidemiologic research designed by the Ministry of Education, Culture, Sports, Science and Technology and Ministry of Health, Labour and Welfare of Japan. The study design was approved by the institutional review board of the University of Tokyo Hospital.

An open-label phase I/II trial of TSU-68 for the treatment of HCC was performed between September 2003 and February 2007 at three institutions in Japan [21]. Twenty-five of the participating patients were enrolled from the University of Tokyo Hospital. In the present study, clinical data for these 25 patients, including analyses conducted before and after the trial, were further evaluated. Briefly, histologically confirmed HCC patients without indication or response to resection, ablation, or transcatheter arterial chemoembolization (TACE) were deemed eligible. The eligibility criteria also included a World Health Organization (WHO) performance status of 2 or better, a life expectancy of not less than 90 days, and a liver function of Child–Pugh class A or B. Patients were not eligible if they had received ablation, TACE, chemotherapy, or irradiation within 4 weeks, or surgery within 6 weeks, of the commencement of the trial (washout phase).

The phase I study began with a 400 mg bid oral dose of TSU-68. Because of dose-limiting toxicities, however, this was reduced to 200 mg bid in the subsequent phase II study. At the end of each 4-week cycle, dynamic contrast-enhanced computed tomography (CT) consisting of early and late arterial, and portal venous phases was performed, and contiguous transverse sections with a thickness of 5 mm were obtained. Responses were assessed on the basis on the RECIST evaluations in predetermined target lesions. The serum levels of HCC-specific tumor markers, AFP and DCP, were scheduled to be determined every 2 weeks. TSU-68 administration was discontinued when progressive disease (PD) was observed by RECIST.

Patients

Among the patients who had participated in the aforementioned trial, those who met the following criteria were included in the present study: (1) tumor growth prior to TSU-68 administration could be evaluated with two CT examinations performed 1–3 months before the trial and upon enrollment; (2) serum tumor marker levels could be determined at least three times during the washout phase, and a linear regression of the logarithmic transformation of marker levels over time showed an r^2 greater than

0.80; and (3) TSU-68 had been administered for at least 4 weeks.

Radiological evaluation of tumor volume

Radiological evaluations were performed according to RECIST guidelines version 1.0 [27]. Not more than 10 lesions, including intrahepatic tumors and extrahepatic metastases, were selected as target lesions prior to TSU-68 administration. In addition to RECIST, we also in our present analyses estimated the volume of each target lesion as a sphere taking the average of its major and minor axes as the diameter [28], and thereby calculating the radiological tumor volume DT as

$$\mathrm{DT} = \log(2) \times \frac{t_2 - t_1}{\log(V_2) - \log(V_1)}$$

where V_1 and V_2 are the volumes at times t_1 and t_2 [29].

Tumor markers

The HCC-specific tumor markers, AFP and DCP, were measured every 2 weeks for each patient registered in the trial. The serum AFP levels were measured via an enzyme immunoassay (ST AIA-PACK AFP, Tosoh, Tokyo, Japan) and DCP was measured using a chemiluminescent enzyme immunoassay (LUMIPULSE PIVKA-II, Eisai, Tokyo, Japan). These markers were also assayed after the termination of TSU-68 treatment, usually with a longer interval.

Tumor marker doubling time

In the present analyses, we assumed that the serum levels of tumor marker are proportional to the viable tumor volume with a fixed coefficient intrinsic to an individual case, when the tumor was producing the marker in question. Independently of the coefficient, the DT values can be calculated from two data points as

$$\mathrm{DT} = \log(2) \times \frac{t_2 - t_1}{\log(C_2) - \log(C_1)}$$

where C_1 and C_2 are the serum concentrations of tumor marker at times t_1 and t_2.

When data were available at more than two points, we first performed linear regression analysis of log-transformed tumor marker levels over time to determine the slope, and the DT was then calculated as

$$\mathrm{DT} = \frac{\log(2)}{\mathrm{slope}}.$$

Note in this case that the DT becomes negative when the tumor marker levels decrease following treatment.

Tumor volume and tumor marker levels during the washout phase

The total volume of target lesions was measured via two CT examinations during the washout phase: one at 4–12 weeks before and another immediately prior to the commencement of TSU-68 treatment. The tumor volume DT was then calculated as described above. The tumor marker DT was also calculated, and the relationship between the two sets of DT values was analyzed.

Changes in the DTs during TSU-68 treatment

The serum tumor marker DT during the first 8 weeks of TSU-68 administration was similarly calculated and compared with the DT measured before the drug therapy. If TSU-68 administration had been effective, the DT should be elongated, or yield a negative value. The evaluation of drug responses based on tumor marker DT was then compared with that by the RECIST method.

Tumor marker DT after the cessation of TSU-68 treatment

When a patient was observed without any anticancer treatment for more than 4 weeks after the cessation of TSU-68 treatment and tumor marker levels were determined more than once during this period, tumor marker DTs after the cessation of TSU-68 were similarly calculated and compared with those measured at 4 weeks and immediately before the cessation of treatment. The study design we used for estimating tumor marker DT before, during, and after TSU-68 administration is summarized in Fig. 1.

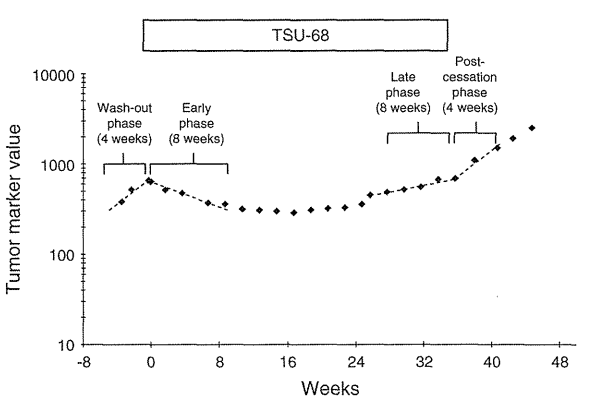

Fig. 1 Linear regression representation of the log tumor marker levels over time where DT = log(2)/slope. The slope can be calculated using a least-squares regression or two log-transformed tumor marker values: DT = log(2) × (t_2 − t_1)/[log(TM2) − log(TM1)], where t = time and TM = tumor marker level

Results

Patient characteristics

Among the 25 patients enrolled at the University of Tokyo Hospital, 15 met all of the inclusion criteria. The reasons for exclusion included insufficient tumor marker determination prior to TSU-68 administration (seven patients), results of CT prior to enrollment unavailable (one patient), no tumor marker elevation (one patient), and termination of TSU-68 administration at week 2 as a result of gastrointestinal bleeding (one patient). The baseline characteristics of the 15 patients included in the current study cohort are summarized in Table 1.

Table 1 Patient characteristics

Variable	$n = 15$
Age (years)	66.7 ± 6.3
Sex [no. (%)]	
Male	12 (80)
Female	3 (20)
Viral markers [no. (%)]	
HBs Ag+, HCV Ab−	2 (13)
HBs Ag−, HCV Ab+	13 (87)
Prior treatments[a] [no. (%)]	
TACE	13 (87)
Ablation	12 (80)
Surgery	5 (33)
Radiation	2 (13)
Systemic chemotherapy	1 (7)
Tumor stage [no. (%)[b]]	
I	0 (0)
II	0 (0)
III	7 (47)
IVa	4 (27)
IVb	4 (27)
Extrahepatic metastasis [no. (%)]	8 (53)
Portal vein thrombosis [no. (%)]	1 (7)

Plus-minus values represent the mean and standard deviation

HBs Ag hepatitis B surface antigen, *HCV Ab* hepatitis C antibody

[a] Number of pretreatments by surgery, radiofrequency ablation, transcatheter arterial chemoembolization, chemotherapy, or radiotherapy

[b] Based on the International Union Against Cancer (UICC) *TNM Classification of Malignant Tumors*, 6th edition, 2002

Tumor volume and tumor marker prior to TSU-68 administration

The relationship between the tumor volume and tumor marker DTs is shown in Fig. 2, where each point represents data from one patient. With the least-square method, the relationship was regressed to

$$y = 1.063x - 2.941$$

where x is the tumor volume DT and y is the tumor marker DT in days for both. The slope of regression was close to 1.0 with an r^2 value of 0.948, indicating that these two DTs were almost identical in each patient.

Changes in tumor marker DT during TSU-68 treatment

TSU-68 treatment was discontinued at week 4 in four patients because of the appearance of new lesions or a substantial increase in the volume of non-target lesions. The remaining 11 patients received this drug for at least 8 weeks and the response of the target lesions was evaluated in these patients as a stable disease (SD) by RECIST at week 4. Changes in the tumor marker DT before and after the commencement of TSU-68 administration are summarized in Table 2, together with the corresponding RECIST evaluation. When the tumor marker DT was increased following TSU-68 therapy, or became negative, this was considered to be an indication of at least partial drug efficacy. On the other hand, no beneficial effects were assigned to TSU-68 when the tumor marker DT was shortened following treatment. Such tumor marker-based evaluations were found to be compatible with RECIST, as a complete or partial response (CR, PR), or SD versus PD, in 12 of 15 patients. In the remaining three patients, a RECIST-based evaluation of PD was obtained in spite of an elongated tumor marker DT. In case 9, the RECIST-based evaluation became PD after cycle 2 because of the appearance of a new lesion, although the tumor marker DT was still elongated in this patient. Lymph node necrosis was observed by contrast-enhanced CT in this patient (Fig. 3), suggesting that TSU-68 remained effective. In case 10, a RECIST-based evaluation of PD was obtained because of an increase in the size of adrenal metastasis (a target lesion) although the hepatic lesions were decreased in size and the tumor marker DT was elongated. After the cessation of TSU-68 in patient 10, the left adrenal gland was excised and found to contain multiple necrotic lesions. Case 12 showed SD for the target lesion and an elongated tumor marker DT but was deemed to be a PD because of the appearance of new lesions.

In two of the other cases (nos. 1 and 2), a RECIST-based evaluation of SD was found but a negative tumor marker DT was also obtained. In case 1, the tumor marker DT became −21.1 days upon TSU-86 administration, which indicated an 84% decrease in tumor volume and 46% reduction in diameter by 8 weeks. Using RECIST parameters, a greater than 30% decrease in diameter typically corresponds to PR but case 1 was nevertheless evaluated as

SD using this system. In case 2, a tumor marker DT of −29.5 days corresponded to a decrease in diameter to 64% of baseline but the RECIST-based evaluation was SD. Importantly, necrotic lesions were found in the target tumors in both cases, possibly leading to an underestimation of anticancer effect.

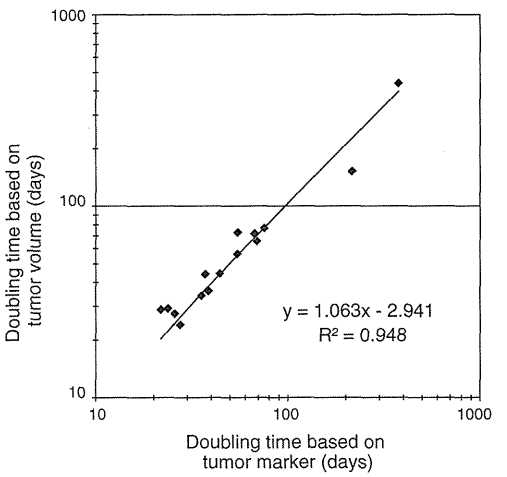

Fig. 2 Linear regression representation of the log tumor volume doubling time over the log tumor marker doubling time. *Each point* represents a data set from a single patient

Changes in tumor marker DT after the cessation of TSU-68 treatment

Changes in tumor marker DTs following the cessation of TSU-68 could be evaluated in four patients (Table 3). In each of these cases, the tumor marker DTs were elongated during TSU-68 administration compared with the baseline value and became shorter after the cessation of the treatment. Tumor marker DT after the cessation of TSU-68 was comparable with that before treatment in three patients and shorter in the remaining case.

Discussion

The production rate of a tumor marker per unit volume of the tumor mass can vary greatly among cancer patients who are positive for this marker. Hence, the serum levels of tumor marker are not directly proportional to the tumor volume. However, provided that the production rate per unit of tumor volume remains constant in each case, the changes in the serum tumor marker levels will directly correspond to the changes in tumor volume. Indeed, as we have shown in the present study, the DT of a tumor marker level and that of the corresponding tumor volume were almost identical in each patient in this study, at least during

Table 2 Tumor marker doubling time and treatment response evaluated by RECIST

Case no.	Marker	Tumor marker levels[a]		Doubling time (days)		Treatment response by RECIST
		At enrollment	At evaluation	During washout phase	During TSU-68 administration	
1	DCP	213	29	136.8	−21.1[b]	SD
2	AFP	60836	15312	38.6	−29.5[b]	SD
3	DCP	5993	5007	26.9	−231.6[b]	SD
4	AFP	144045	134030	75.3	−602.1[b]	SD
5	AFP	12004	12010	18.8	43004	SD
6	AFP	33859	33983	24.1	3010	SD[c]
7	AFP	61649	88056	71.7	115.8	SD
8	AFP	198	395	51.9	60.2	SD
9	AFP	45	92	28.0	60.2	PD
10	DCP	657	997	38.1	51.0	PD[c]
11	DCP	3188	8275	54.7	43.6	PD
12	AFP	3404	6430	24.7	32.4	PD[c]
13	AFP	53	203	88.5	15.5	PD[c]
14	AFP	19	544	376.3	12.4	PD
15	AFP	30	169	25.7	12.0	PD[c]

AFP alpha-fetoprotein, *DCP* des-gamma carboxyprothrombin, *SD* stable disease, *PD* progressive disease

[a] Unit of AFP is ng/ml and unit of DCP is mAu/ml

[b] Became negative when the tumor marker levels decreased following treatment; negative DT values correspond to the half-life

[c] Calculated using the values obtained at week 4 as treatment was discontinued at this time point. The treatment response evaluations using RECIST were also performed at week 4

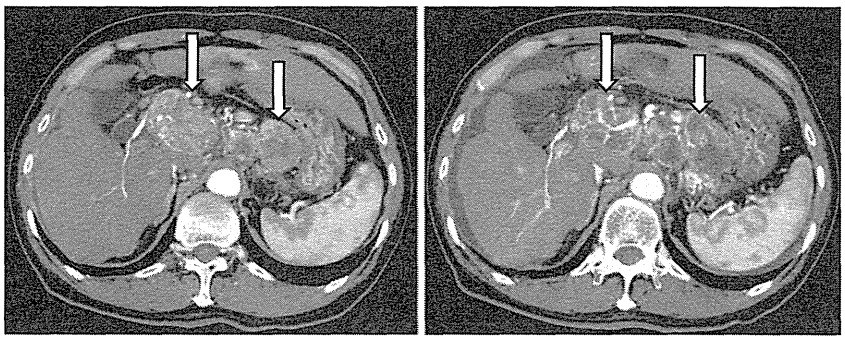

Fig. 3 A case in which a RECIST evaluation of PD was obtained even though the tumor marker levels had decreased. The lymph nodes around the hepatic arteries (target lesions, *arrows*) in this patient were enlarged and had become internally necrotic

Table 3 Tumor marker doubling time (days) before, during, and after TSU-68 treatment

Case no.	During washout phase	During the first 4 weeks of administration	During the last 4 weeks of administration	After cessation of administration
3	26.9	−97.1[b]	91.2	41.2
4	75.3	−79.2[b]	188.1	17.8
6[a]	24.1	3010	–	46.3
9	28.0	60.2	60.2	35.4

[a] Treatment was discontinued at week 4

[b] Became negative when the tumor marker levels decreased following treatment

washout phase prior to TSU-68 therapy. This indicates the possibility that tumor growth rates and any changes in them can be evaluated using tumor marker DT.

To validate the usefulness of tumor marker DTs for evaluating treatment responses, we compared this approach with the RECIST guidelines during TSU-68 administration. These two methods showed comparable results in most cases (12/15) and discrepancies were due to substantial tumor necrosis without volume shrinkage or to the appearance of new lesions in spite of the sustained effects of the drug on the target lesions. Tumor marker levels can be considered to represent viable tumor burden irrespective of the presence of necrosis or fibrosis. Evaluations based on tumor marker DTs may thus provide a better assessment of the efficacy of chemotherapeutic agents. Modified RECIST was proposed after the protocol of this study was completed. In modified RECIST, only areas with hyperattenuation were measured, excluding necrotic tissues. Modified RECIST was reported to be more useful than conventional RECIST in the evaluation of antiangiogenic agents. Although we did not directly compare tumor DT with modified RECIST in the present study, assessment based on tumor DT may be closer to modified RECIST than to conventional RECIST.

In several previous papers, early changes in AFP levels were used to assess responses to HCC treatments [30–32]. However, they evaluated only initial responses to therapy. In contrast, by evaluating tumor DT based on tumor marker levels, the effectiveness of a therapeutic agent can be monitored during its administration even when it changes over time.

In previous phase III trials of sorafenib, the response rate was not high but the overall survival was significantly improved [33, 34]. Slowing down the progression of a tumor, even if there is no reduction in the tumor volume, can therefore lead to prolonged survival. In the present study, the tumor marker DT was shortened after the cessation of TSU-68 treatment in four patients, i.e., tumor growth was accelerated, indicating that TSU-68 still inhibited tumor growth. Using RECIST evaluation, however, the treatment response in such cases will be judged as a PD, because this method does not consider time. Hence, in evaluating the response to cytostatic agents in particular, such as sorafenib and TSU-68, determination of the changes in the tumor growth rate may be substantially more adequate. Tumor marker levels can be easily measured repeatedly and, as shown in the current analysis, the corresponding DTs can thus be reliably calculated. Theoretically, the serum half-life of a tumor marker may affect the calculation of tumor DT. However, the half-life of AFP is 5 days and that of DCP is 40 h, which are much shorter than the tumor halving time even when TSU-68 is effective, and are negligible in calculations.

Another application of tumor marker DTs is the estimation of tumor growth rates when the lesions are untreated. DTs may correlate with the malignant potential of the tumor. We have shown that tumor marker DTs remained similar before the administration and after the cessation of TSU-68, which may be a characteristic of cytostatic agents in contrast to cytotoxic agents [35–37]. The decision to continue cytotoxic agents that only slow down tumor growth could be partially based on the tumor marker DT prior to treatment.

There are several limitations to the use of tumor marker DTs in the evaluation of cancer drug treatment responses. First, DTs cannot be calculated when a tumor does not produce tumor markers. Second, a tumor marker profile may change during treatment, possibly as a result of somatic mutation and clonal selection in the tumor cell population. This may make interpretation of changes in DTs difficult. Lastly, whether an elongated but still positive DT is associated with improved prognosis has yet to be confirmed. In the natural course of HCC, the tumor volume DT has been reported to be associated with prognosis [38]. We thus speculate that a treatment associated with elongation of tumor marker DT can be continued if there are no alternative treatments and the side effects are tolerable.

In conclusion, we have shown that serum tumor marker levels can be used to evaluate viable tumor burden irrespective of the presence of tumor necrosis that can compromise radiographic evaluations. This may be particularly useful in the evaluation of cytostatic agents.

Conflict of interest The authors declare that they have no conflict of interest.

References

1. Cannistra SA. Phase II trials in *Journal of Clinical Oncology*. J Clin Oncol. 2009;27:3073–6.
2. Paesmans M, Sculier JP, Libert P, Bureau G, Dabouis G, Thiriaux J, et al. Response to chemotherapy has predictive value for further survival of patients with advanced non-small cell lung cancer: 10 years experience of the European Lung Cancer Working Party. Eur J Cancer. 1997;33:2326–32.
3. Buyse M, Thirion P, Carlson RW, Burzykowski T, Molenberghs G, Piedbois P. Relation between tumour response to first-line chemotherapy and survival in advanced colorectal cancer: a meta-analysis. Meta-Analysis Group in Cancer. Lancet. 2000;356: 373–8.
4. Goffin J, Baral S, Tu D, Nomikos D, Seymour L. Objective responses in patients with malignant melanoma or renal cell cancer in early clinical studies do not predict regulatory approval. Clin Cancer Res. 2005;11:5928–34.
5. Keppke AL, Salem R, Reddy D, Huang J, Jin J, Larson AC, et al. Imaging of hepatocellular carcinoma after treatment with yttrium-90 microspheres. AJR Am J Roentgenol. 2007;188: 768–75.
6. Miller FH, Keppke AL, Reddy D, Huang J, Jin J, Mulcahy MF, et al. Response of liver metastases after treatment with yttrium-90 microspheres: role of size, necrosis, and PET. AJR Am J Roentgenol. 2007;188:776–83.
7. Burton A. REGIST: right time to renovate? Eur J Cancer. 2007;43:1642.
8. Therasse P, Eisenhauer EA, Buyse M. Update in methodology and conduct of cancer clinical trials. Eur J Cancer. 2006;42: 1322–30.
9. Therasse P, Eisenhauer EA, Verweij J. RECIST revisited: a review of validation studies on tumour assessment. Eur J Cancer. 2006;42:1031–9.
10. Stroobants S, Goeminne J, Seegers M, Dimitrijevic S, Dupont P, Nuyts J, et al. 18FDG-positron emission tomography for the early prediction of response in advanced soft tissue sarcoma treated with imatinib mesylate (Glivec). Eur J Cancer. 2003;39:2012–20.
11. Antoch G, Kanja J, Bauer S, Kuehl H, Renzing-Koehler K, Schuette J, et al. Comparison of PET, CT, and dual-modality PET/CT imaging for monitoring of imatinib (STI571) therapy in patients with gastrointestinal stromal tumors. J Nucl Med. 2004;45:357–65.
12. D'Amico AV, Desjardin A, Chen MH, Paik S, Schultz D, Renshaw AA, et al. Analyzing outcome-based staging for clinically localized adenocarcinoma of the prostate. Cancer. 1998;83:2172–80.
13. Sheu JC, Sung JL, Chen DS, Yang PM, Lai MY, Lee CS, et al. Growth rate of asymptomatic hepatocellular carcinoma and its clinical implications. Gastroenterology. 1985;89:259–66.
14. Tian F, Appert HE, Myles J, Howard JM. Prognostic value of serum CA 19-9 levels in pancreatic adenocarcinoma. Ann Surg. 1992;215:350–5.
15. Tanaka K, Noura S, Ohue M, Seki Y, Yamada T, Miyashiro I, et al. Doubling time of carcinoembryonic antigen is a significant prognostic factor after the surgical resection of locally recurrent rectal cancer. Dig Surg. 2008;25:319–24.
16. Stamey TA, Kabalin JN, Ferrari M. Prostate specific antigen in the diagnosis and treatment of adenocarcinoma of the prostate. III. Radiation treated patients. J Urol. 1989;141:1084–7.
17. Stamey TA, Kabalin JN, Ferrari M, Yang N. Prostate specific antigen in the diagnosis and treatment of adenocarcinoma of the prostate. IV. Anti-androgen treated patients. J Urol. 1989;141: 1088–90.
18. Stamey TA, Kabalin JN, McNeal JE, Johnstone IM, Freiha F, Redwine EA, et al. Prostate specific antigen in the diagnosis and treatment of adenocarcinoma of the prostate. II. Radical prostatectomy treated patients. J Urol. 1989;141:1076–83.
19. Fabbro D, Manley PW. Su-6668. SUGEN. Curr Opin Investig Drugs. 2001;2:1142–8.
20. Pang RW, Poon RT. From molecular biology to targeted therapies for hepatocellular carcinoma: the future is now. Oncology. 2007;72(Suppl 1):30–44.
21. Kanai F, Yoshida H, Tateishi R, Sato S, Kawabe T, Obi S, et al. A phase I/II trial of the oral antiangiogenic agent TSU-68 in patients with advanced hepatocellular carcinoma. Cancer Chemother Pharmacol. 2011;67:315–24.
22. Eisenhauer EA. Phase I and II trials of novel anti-cancer agents: endpoints, efficacy and existentialism. The Michel Clavel Lecture, held at the 10th NCI-EORTC Conference on New Drugs in Cancer Therapy, Amsterdam, 16–19 June 1998. Ann Oncol. 1998;9:1047–52.
23. Eisenhauer EA. Response evaluation: beyond RECIST. Ann Oncol. 2007;18 Suppl 9:ix29–32.
24. Gelmon KA, Eisenhauer EA, Harris AL, Ratain MJ, Workman P. Anticancer agents targeting signaling molecules and cancer cell environment: challenges for drug development? J Natl Cancer Inst. 1999;91:1281–7.
25. Korn EL, Arbuck SG, Pluda JM, Simon R, Kaplan RS, Christian MC. Clinical trial designs for cytostatic agents: are new approaches needed? J Clin Oncol. 2001;19:265–72.
26. Ratain MJ, Eckhardt SG. Phase II studies of modern drugs directed against new targets: if you are fazed, too, then resist RECIST. J Clin Oncol. 2004;22:4442–5.
27. Therasse P, Arbuck SG, Eisenhauer EA, Wanders J, Kaplan RS, Rubinstein L, et al. New guidelines to evaluate the response to treatment in solid tumors European Organization for Research and Treatment of Cancer, National Cancer Institute of the United States, National Cancer Institute of Canada. J Natl Cancer Inst. 2000;92:205–16.
28. Dachman AH, MacEneaney PM, Adedipe A, Carlin M, Schumm LP. Tumor size on computed tomography scans: is one measurement enough? Cancer. 2001;91:555–60.

29. Schwartz M. A biomathematical approach to clinical tumor growth. Cancer. 1961;14:1272–94.
30. Chan SL, Mo FK, Johnson PJ, Hui EP, Ma BB, Ho WM, et al. New utility of an old marker: serial alpha-fetoprotein measurement in predicting radiologic response and survival of patients with hepatocellular carcinoma undergoing systemic chemotherapy. J Clin Oncol. 2009;27:446–52.
31. Riaz A, Ryu RK, Kulik LM, Mulcahy MF, Lewandowski RJ, Minocha J, et al. Alpha-fetoprotein response after locoregional therapy for hepatocellular carcinoma: oncologic marker of radiologic response, progression, and survival. J Clin Oncol. 2009;27:5734–42.
32. Shao YY, Lin ZZ, Hsu C, Shen YC, Hsu CH, Cheng AL. Early alpha-fetoprotein response predicts treatment efficacy of antiangiogenic systemic therapy in patients with advanced hepatocellular carcinoma. Cancer. 2010;116:4590–6.
33. Llovet JM, Ricci S, Mazzaferro V, Hilgard P, Gane E, Blanc JF, et al. Sorafenib in advanced hepatocellular carcinoma. N Engl J Med. 2008;359:378–90.
34. Cheng AL, Kang YK, Chen Z, Tsao CJ, Qin S, Kim JS, et al. Efficacy and safety of sorafenib in patients in the Asia-Pacific region with advanced hepatocellular carcinoma: a phase III randomised, double-blind, placebo-controlled trial. Lancet Oncol. 2009;10:25–34.
35. Bourhis J, Wilson G, Wibault P, Janot F, Bosq J, Armand JP, et al. Rapid tumor cell proliferation after induction chemotherapy in oropharyngeal cancer. Laryngoscope. 1994;104:468–72.
36. Davis AJ, Tannock JF. Repopulation of tumour cells between cycles of chemotherapy: a neglected factor. Lancet Oncol. 2000;1:86–93.
37. Kim JJ, Tannock IF. Repopulation of cancer cells during therapy: an important cause of treatment failure. Nat Rev Cancer. 2005;5:516–25.
38. Okazaki N, Yoshino M, Yoshida T, Suzuki M, Moriyama N, Takayasu K, et al. Evaluation of the prognosis for small hepatocellular carcinoma based on tumor volume doubling time. A preliminary report. Cancer. 1989;63:2207–10.

nature immunology

Tumor-infiltrating DCs suppress nucleic acid–mediated innate immune responses through interactions between the receptor TIM-3 and the alarmin HMGB1

Shigeki Chiba[1], Muhammad Baghdadi[1–3], Hisaya Akiba[4], Hironori Yoshiyama[1], Ichiro Kinoshita[3], Hirotoshi Dosaka-Akita[3], Yoichiro Fujioka[5], Yusuke Ohba[5], Jacob V Gorman[6], John D Colgan[6], Mitsuomi Hirashima[7], Toshimitsu Uede[8], Akinori Takaoka[2], Hideo Yagita[4] & Masahisa Jinushi[1]

© 2012 Nature America, Inc. All rights reserved.

The mechanisms by which tumor microenvironments modulate nucleic acid–mediated innate immunity remain unknown. Here we identify the receptor TIM-3 as key in circumventing the stimulatory effects of nucleic acids in tumor immunity. Tumor-associated dendritic cells (DCs) in mouse tumors and patients with cancer had high expression of TIM-3. DC-derived TIM-3 suppressed innate immune responses through the recognition of nucleic acids by Toll-like receptors and cytosolic sensors via a galectin-9-independent mechanism. In contrast, TIM-3 interacted with the alarmin HMGB1 to interfere with the recruitment of nucleic acids into DC endosomes and attenuated the therapeutic efficacy of DNA vaccination and chemotherapy by diminishing the immunogenicity of nucleic acids released from dying tumor cells. Our findings define a mechanism whereby tumor microenvironments suppress antitumor immunity mediated by nucleic acids.

Accumulating evidence has demonstrated the potential of endogenous immune responses in modulating the clinical outcome of malignant diseases[1,2]. Thus, manipulation of the immune system should enable enhancement of the therapeutic effects of the present anticancer modalities[3,4]. However, oncogenic and epigenetic alterations of tumor cells often adopt multiple strategies to form complex networks with tumor-infiltrating cells, which leads to the impairment of efficient tumor immunosurveillance[5,6].

Innate immunity serves as a first line of defense against infectious agents, and germline-encoded pattern-recognition receptors (PRRs) detect stressed and infected cells and elicit potent effector activities that achieve efficient containment of microbes[7]. Among the specialized subsets of cells of the innate immune system, dendritic cells (DCs) are particularly important as critical sensors through their wide expression of various PRRs[8]. These pattern-sensing systems on DCs are also applicable to the recognition of tumor-derived stress-related factors. In particular, Toll-like receptors (TLRs) and cytosolic sensors for DNA and RNA recognition expressed by DCs use endogenous host elements carrying microbial components (such as the alarmin HMGB1), pathogen-associated molecular patterns and/or nucleic acids to stimulate intrinsic apoptotic pathways to generate protective immune responses to nascent tumors[9–11]. However, how DCs regulate PRR-mediated innate immune systems in tumor microenvironments and thus how they affect anticancer therapies remain largely unknown.

Here we identify the receptor TIM-3 on DCs as a key factor in circumventing nucleic acid–mediated activation of the innate immune system. TIM-3 was initially identified as a negative regulator of T helper type 1 immunity after ligation of galectin-9 (refs. 12–14). However, TIM-3 is also expressed on myeloid cells such as monocytes and macrophages[15,16], but whether TIM-3 on DCs has a role in the regulation of antitumor immunity has remained largely unknown. We found here that DCs in tumor microenvironments had higher expression of TIM-3 than did DCs in normal tissues. Furthermore, TIM-3 on tumor-associated DCs (TADCs) suppressed PRR-mediated innate immune responses to nucleic acids by interfering with HMGB1-mediated activation of nucleic acid–sensing systems. Our findings define a mechanism by which tumor microenvironments impede the immunological responses of DCs to nucleic acid adjuvants, which results in impaired antitumor immunosurveillance and therapy.

RESULTS

High expression of TIM-3 by tumor-infiltrating DCs

To explore a potential role for TIM-3 in regulating antitumor responses, we examined its expression on myeloid cells from mice bearing 3LL

[1]Research Center for Infection-Associated Cancer, Institute for Genetic Medicine, Hokkaido University, Sapporo, Japan. [2]Division of Signaling on Cancer and Immunology, Institute for Genetic Medicine, Hokkaido University, Sapporo, Japan. [3]Department of Medical Oncology, Hokkaido University Graduate School of Medicine, Sapporo, Japan. [4]Department of Immunology, Juntendo University School of Medicine, Tokyo, Japan. [5]Department of Pathophysiology and Signal Transduction, Hokkaido University Graduate School of Medicine, Sapporo, Japan. [6]Department of Internal Medicine, University of Iowa, Iowa City, Iowa, USA. [7]Department of Immunology and Immunopathology, Faculty of Medicine, Kagawa University, Kagawa, Japan. [8]Division of Molecular Immunology, Institute for Genetic Medicine, Hokkaido University, Sapporo, Japan. Correspondence should be addressed to M.J. (jinushi@igm.hokudai.ac.jp).

Received 15 May; accepted 19 June; published online 29 July 2012; doi:10.1038/ni.2376

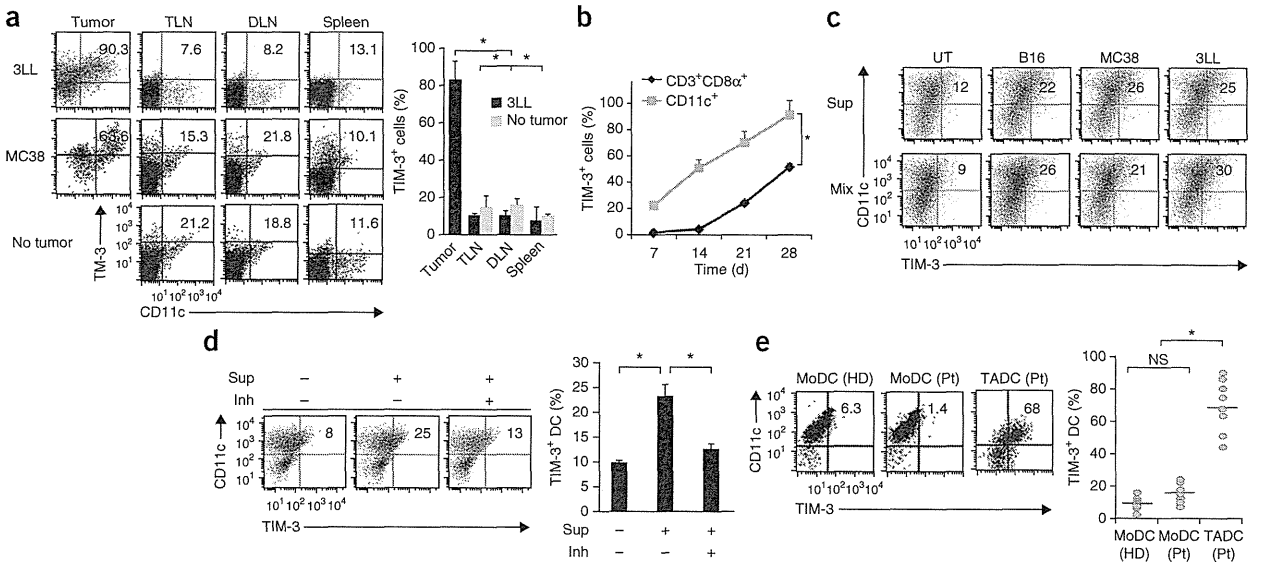

Figure 1 Expression of TIM-3 on TADCs. (**a**) TIM-3 expression by DCs from established tumors (Tumor), tumor-draining lymph nodes (TLN), distal lymph nodes (DLN) or spleens of mice bearing 3LL or MC38 tumors at 28 d after tumor inoculation, and from tumor-free mice (No tumor; control), analyzed by flow cytometry (left). Numbers in top right quadrants indicate percent TIM-3$^+$CD11c$^+$ cells. Right, TIM-3$^+$ cells among CD11c$^+$ cells isolated from mice bearing 3LL tumors or no tumors (average). (**b**) Longitudinal analysis of TIM-3-expressing CD11c$^+$ DCs or CD3$^+$CD8$^+$ T cells (Cd3$^+$CD8α$^+$) after inoculation of 3LL tumors. (**c**) TIM-3 expression by BMDCs left untreated (UT) or treated for 48 h with supernatants of B16, MC38 or 3LL tumor cells (20% in total medium; Sup) or cultured for 48 h together with those tumor cells (Mix), evaluated by flow cytometry (numbers in plots as in **a**). (**d**) TIM-3 expression on BMDCs left untreated (Sup –) or treated for 48 h with supernatants of 3LL cell cultures (Sup +) left untreated (Inh –) or treated with anti-VEGF-R2, anti-IL-10 and inhibitor of arginase I (Inh +), evaluated by flow cytometry (left; numbers in plots as in **a**). Right, frequency of TIM-3$^+$CD11c$^+$ DCs. (**e**) TIM-3 expression on DCs differentiated from peripheral blood monocytes (MoDCs) from healthy donors (HD; $n = 7$) or patients with cancer (Pt; $n = 7$), and TADCs from those same patients ($n = 9$), evaluated by flow cytometry (left; numbers in plots as in **a**). Right, frequency of TIM-3$^+$CD11c$^+$ DCs; each symbol represents an individual donor, and small horizontal lines indicate the mean. NS, not significant. $^*P < 0.05$ (paired Student's *t*-test). Data are representative of four experiments (**a**–**d**; error bars (**a**,**b**,**d**), s.e.m.) or three experiments (**e**).

© 2012 Nature America, Inc. All rights reserved.

Lewis lung cancer tumors or MC38 colorectal adenocarcinoma tumors. Among single-cell suspensions prepared from subcutaneous tumors, CD11c^{hi} conventional DCs, CD11c^{lo}B220$^+$PDCA1$^+$ plasmacytoid DCs and CD11b$^+$F4/80$^+$ tumor-associated macrophages had high TIM-3 expression, but CD11b$^+$Gr-1$^+$ myeloid-derived suppressor cells did not (**Fig. 1a** and **Supplementary Fig. 1a**). In contrast, few TIM-3-expressing DCs or macrophages were present in the tumor-draining or distal lymph nodes and spleens of tumor-bearing mice or in mice without tumors (**Fig. 1a**). In line with tumor-specific expression of TIM-3, we also detected TIM-3 on tumor cells *in situ* and tumor-infiltrating CD8$^+$ T cells but not on splenic CD8$^+$ T cells of tumor-bearing mice. In contrast, we did not detect TIM-3 on mouse tumor cell lines cultured *in vitro* (**Supplementary Fig. 1b,c**), which indicated that tumor microenvironments may have a role in the regulation of TIM-3 expression on both the tumor and host leucocytes. However, TIM-3 was expressed on *in vitro*–cultured human non-small-cell lung carcinoma (NSCLC) tumor lines and primary EpCAM$^+$ NSCLC epithelial tumor cells from patients with cancer (**Supplementary Fig. 1d,e**). TIM-3 had much higher expression and was expressed at earlier times on TADCs than on tumor-infiltrating CD8$^+$ T cells after subcutaneous tumor challenge (**Fig. 1b**). In contrast, TIM-3 expression in CD8$^+$ T cells gradually increased and reached its maximum of about 50% of that in total CD8$^+$ T cells by 4 weeks after tumor challenge (**Fig. 1b**). These results suggested that the tumor microenvironment induced DCs to express TIM-3 with kinetics different from those of CD8$^+$ T cells.

To investigate possible tumor-derived factors that contributed to the high expression of TIM-3 by DCs, we incubated immature bone marrow–derived dendritic cells (BMDCs) overnight with mouse tumor cells or with tumor-cell supernatants. TIM-3 expression was much higher after coculture with tumor cells or treatment with culture supernatants than after culture in medium alone (**Fig. 1c,d**). Various factors derived mainly from tumor cells and their microenvironments bestow tumorigenic activities on DCs by inducing their expression of tumor-promoting and immunosuppressive factors, such as arginase I, indoleamine 2,3-deoxygenase, interleukin 10 (IL-10), transforming growth factor-β1 (TGF-β1) and vascular endothelial growth factor (VEGF)[17–19]. Although 3LL tumors treated individually with inhibitors of the VEGF receptor VEGF-R2, IL-10 or arginase I had marginal inhibitory effects on TIM-3 expression when added to BMDCs (**Supplementary Fig. 2a**), treatment with a combination of all three inhibitors largely diminished the upregulation of TIM-3 on BMDCs mediated by tumor-cell supernatants (**Fig. 1d**). Moreover, TIM-3 on BMDCs was upregulated substantially by recombinant IL-10 or VEGF-A alone or together, in a dose-dependent manner (**Supplementary Fig. 2b**).

In contrast to the results noted above, TIM-3 was not upregulated on mouse 3LL NSCLC tumor cells treated with VEGF-A and IL-10 (**Supplementary Fig. 2c**), which suggested that tumor cells use mechanisms to induce their expression of TIM-3 distinct from those used by DCs. Thus, TIM-3 expression on DCs was regulated by the synergistic actions of multiple immunoregulatory factors released from tumor cells. In addition, we also detected high expression of TIM-3 on the surface of CD11c$^+$ TADCs from patients with advanced NSCLC, gastric adenocarcinoma or neuroendocrine tumors but not on DCs differentiated from peripheral blood monocytes of patients or healthy volunteers (**Fig. 1e**). Thus, we detected high expression of TIM-3 specifically on DCs from both mouse and human tumor microenvironments.

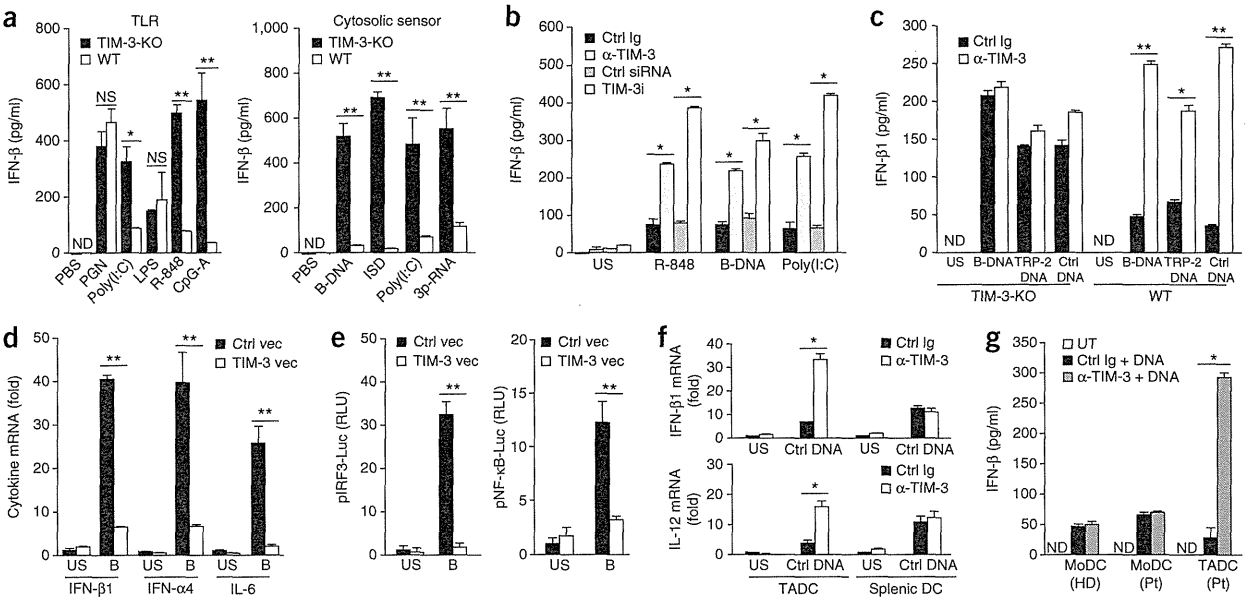

Figure 2 TIM-3 suppresses innate responses to nucleic acids. (**a**) Enzyme-linked immunosorbent assay (ELISA) of IFN-β in wild-type TIM-3$^+$ BMDCs (WT) or TIM-3-deficient TIM-3$^-$ BMDCs (TIM-3-KO) stimulated with PBS or various TLR ligands (left: peptidoglycan (PGN), poly(I:C), lipopolysaccharide (LPS), R-848 or CpG ODN1585 (CpG-A)) or agonists of cytosolic sensors (right: B-DNA, interferon-stimulatory DNA (ISD), poly(I:C) or triphosphate RNA (3p-RNA)). (**b**) ELISA of IFN-β1 in wild-type TIM-3$^+$ DCs treated with control immunoglobulin (Ctrl Ig), mAb to TIM-3 (α-TIM-3), control small interfering RNA (Ctrl siRNA) or small interfering RNA specific for TIM-3 (TIM-3i), followed by no stimulation (unstimulated (US)) or stimulation for 8 h with PBS, R-848, B-DNA or poly(I:C). (**c**) ELISA of IFN-β1 in wild-type TIM-3$^+$ or TIM-3-deficient TIM-3$^-$ BMDCs pretreated with control immunoglobulin or mAb to TIM-3, followed by no stimulation or stimulation for 12 h with B-DNA, plasmid encoding TRP-2 (TRP-2 DNA) or plasmid without insert (Ctrl DNA). (**d**) Quantification of IFN-β1, IFN-α4 and IL-6 mRNA in MEFs transfected for 24 h with control vector (Ctrl vec) or vector encoding TIM-3 (TIM-3 vec), followed by no stimulation or stimulation for 8 h with B-DNA (B); results are presented relative to the expression of *Actb* (reference gene encoding β-actin). (**e**) Luciferase activity in lysates of HEK293T cells transfected and treated as in **d**, assessing the activity of IRF3 (pIRF3-Luc) or NF-κB (pNF-κB-Luc); results are presented in relative light units (RLU) relative to the activity of renilla luciferase. (**f**) RT-PCR quantification of IFN-β1 and IL-12 mRNA in TADCs and splenic DCs isolated from tumor-bearing mice treated with control immunoglobulin or mAb to TIM-3, followed by no stimulation or stimulation for 8 h with plasmid DNA (Ctrl DNA); results are presented relative to *Actb* expression. (**g**) ELISA of IFN-β in DCs differentiated from peripheral blood monocytes from healthy donors or patients with NSCLC, and TADCs from those same patients, left untreated or pretreated with control immunoglobulin or mAb to TIM-3, followed by stimulation with B-DNA (+ DNA). $^*P < 0.05$ and $^{**}P < 0.01$ (paired Student's *t*-test). Data are representative of five experiments (**a**), four experiments (**b**,**c**) or three experiments (**d**–**g**; error bars, s.e.m.).

© 2012 Nature America, Inc. All rights reserved.

TIM-3 suppresses innate responses to nucleic acids

We next evaluated the role of TIM-3 in DC function. For this, we isolated the TIM-3$^+$ population of bulk BMDCs, as TIM-3 is expressed on only a small portion (~5–10%) of BMDCs differentiated with granulocyte-monocyte colony-stimulating factor. TIM-3$^+$ DC populations included more mature CD11c^{hi}CD86^{hi} cells than did their TIM3$^-$ counterparts. However, their ability to cross-prime ovalbumin-specific T cells was similar to that of the TIM-3$^-$ DCs (data not shown).

Given reports indicating that TIM-3 on antigen-presenting cells acts together with TLR signals to trigger inflammatory signals[15], we examined the role of TIM-3 in the regulation of TLR-mediated innate immune responses. Expression of the cytokines interferon-β1 (IFN-β1), IFN-α4, IL-6 and IL-12 was much lower in TIM-3$^+$ DCs isolated from wild-type BMDCs than in TIM-3$^-$ DCs isolated from TIM-3-deficient BMDCs after stimulation with nucleic-acid agonists for TLR3 (the synthetic RNA duplex poly(I: C)), TLR7 (the synthetic imidazoquinoline resiquimod (R-848)) and TLR9 (the dinucleotide CpG-ODN) but not after stimulation with agonists for TLR2 (peptidoglycan) or TLR4 (lipopolysaccharide; **Fig. 2a** and **Supplementary Fig. 3a**). As TLR3, TLR7 and TLR9 serve as pattern-recognition sensors for double-stranded RNA, single-stranded RNA and single-stranded DNA, respectively, we hypothesized that TIM-3 might be broadly involved in the regulation of nucleic acid–mediated immune responses. Indeed, cytokine secretion by wild-type TIM-3$^+$ BMDCs was much lower than that by TIM-3-deficient TIM-3$^-$ BMDCs after stimulation via transfection of synthetic B-form double-stranded DNA (poly(dA:dT); B-DNA) or interferon-stimulatory DNA, which are ligands for sensors of cytosolic DNA, as well as after stimulation with poly(I:C) or triphosphate RNA, which are ligands for the RNA sensors Mda5 and RIG-I (**Fig. 2a**). Moreover, treatment with monoclonal antibody (mAb) to TIM-3 or small interfering RNA targeting TIM-3 expression resulted in much more IFN-β protein in wild-type TIM-3$^+$ DCs in response to agonists for cytosolic sensors or TLRs (**Fig. 2b**). Blockade of TIM-3 also augmented IFN-β1 expression in TIM-3$^+$ DCs derived from wild-type mice, but not those from TIM-3-deficient mice, after treatment with plasmid encoding either of the melanoma-differentiation antigens TRP-2 or gp100 or plasmid with no insert (**Fig. 2c** and data not shown), which indicated that the tumor antigen–encoding sequence was dispensable for the DNA-induced innate immune responses.

To delineate the contribution of TIM-3 to nucleic acid–mediated innate immune responses, we transfected TIM-3$^-$ mouse embryonic fibroblasts (MEFs) with control vector or vector expressing TIM-3. TIM-3 expression led to less cytokine production by MEFs in response to B-DNA, genomic DNA isolated from tumors (B16 mouse melanoma or EL-4 mouse lymphoma) or pathogens, including

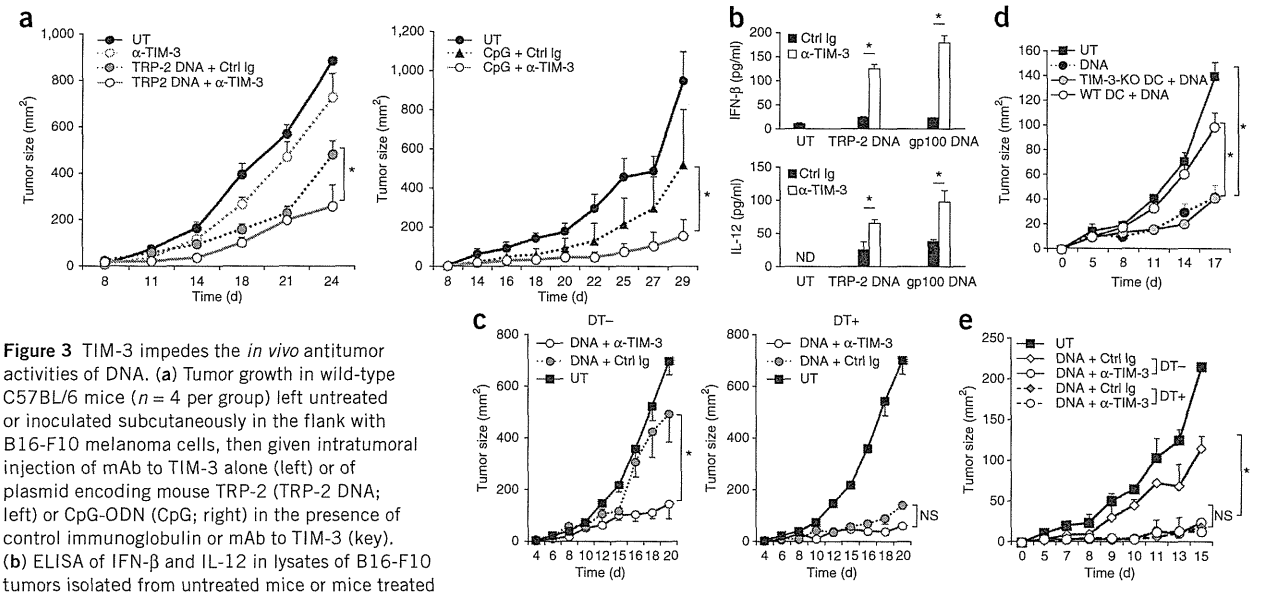

Figure 3 TIM-3 impedes the *in vivo* antitumor activities of DNA. (**a**) Tumor growth in wild-type C57BL/6 mice ($n = 4$ per group) left untreated or inoculated subcutaneously in the flank with B16-F10 melanoma cells, then given intratumoral injection of mAb to TIM-3 alone (left) or of plasmid encoding mouse TRP-2 (TRP-2 DNA; left) or CpG-ODN (CpG; right) in the presence of control immunoglobulin or mAb to TIM-3 (key). (**b**) ELISA of IFN-β and IL-12 in lysates of B16-F10 tumors isolated from untreated mice or mice treated with plasmid encoding TRP-2 or gp100 in the presence of control immunoglobulin or mAb to TIM-3 (key). (**c**) Tumor growth in CD11c-DTR mice given no treatment with diphtheria toxin (DT−) or treated with diphtheria toxin (DT+), then left untreated or inoculated subcutaneously with B16-F10 melanoma cells (1×10^5 cells per mouse) along with control plasmid DNA in the presence of mAb to TIM-3 or isotype-matched control immunoglobulin. (**d**) Tumor growth in diphtheria toxin–treated CD11c-DTR mice ($n = 5$ per group) given no treatment (UT), control plasmid alone (DNA) or adoptive transfer of DCs derived from wild-type or TIM-3-deficient bone marrow, along with intratumoral injection of control plasmid DNA into established B16-F10 tumors. (**e**) Tumor growth in chimeras reconstituted with a mixture of bone marrow cells from TIM-3-deficient mice and CD11c-DTR mice given no treatment with diphtheria toxin or treated with diphtheria toxin 2 d before inoculation with B16-F10 tumor cells (1×10^5 cells per mouse), then left untreated (UT) or treated 8, 10 and 12 d later with control plasmid DNA in the presence of isotype-matched control immunoglobulin or mAb to TIM-3 after tumor inoculation. $^*P < 0.05$ (paired Student's *t*-test). Data are representative of four experiments (**a**), three experiments (**b**,**c**), two independent experiments (**d**) or two experiments (**e**; error bars, s.e.m.).

Escherichia coli, *Helicobacter pylori* and human cytomegalovirus (**Fig. 2d** and **Supplementary Fig. 3b**). We also observed TIM-3-mediated suppression of innate responses to bacterial and viral DNA in BMDCs (data not shown). Moreover, luciferase reporter assays of HEK293 human embryonic kidney cells showed that TIM-3 suppressed the B-DNA-induced activity of the transcription factors IRF3 and NF-κB, which serve as essential components of TLR- and cytosolic sensor–mediated responses (**Fig. 2e**).

To determine whether TIM-3 negatively regulated innate immune responses to nucleic acids *in vivo*, we measured IFN-β1 mRNA and IL-12 mRNA in TADCs isolated from tumor-bearing mice or patients with cancer. TADCs had a lower abundance of transcripts for IFN-β1 and IL-12 and less secretion IFN-β1 and IL-12 protein induced by control plasmid with no insert (empty vector; called 'control plasmid DNA' here) than did splenic DCs or DCs differentiated from peripheral blood monocytes, but treatment with mAb to TIM-3 resulted in higher cytokine expression and more release of cytokines to an even greater degree in TADCs than in splenic DCs or DCs differentiated from peripheral blood monocytes (**Fig. 2f,g**).

Consistent with a critical role for DC-derived TIM-3 in restraining immune responses to nucleic acids, TIM-3 strongly suppressed cytokine production by $CD11c^{lo}B220^+$ plasmacytoid DCs in a manner similar to that seen with $CD11c^{hi}$ conventional DCs infiltrating into tumor tissue. The upregulation of the expression of IFN-β and IL-12 mediated by mAb to TIM-3 was much greater in $CD11c^{hi}$ DCs or $CD11c^{lo}B220^+$ plasmacytoid DCs than in tumor-associated macrophages or myeloid-derived suppressor cells isolated from tumor tissue, whereas upregulation of the expression of TIM-3 was similar among these cells of the myeloid lineage (**Supplementary Figs. 1a** and **3c**). Blockade of TIM-3 had little effect on innate responses in $TIM\text{-}3^{hi}$ tumor-infiltrating $CD8^+$ T cells after stimulation with CpG-ODN (data not shown). Together these results demonstrated that TIM-3 resulted in much less activation of TADCs by interfering with their recognition of and response to normally immunostimulatory nucleic acids.

DC-specific TIM-3 perturbs the antitumor efficacy of DNA

To examine the effect of TIM-3 on nucleic acid–mediated antitumor responses, we used various nucleic acid–based adjuvants, including control plasmid DNA or plasmid encoding TRP-2 (ref. 20), as well as the TLR9 agonist CpG-ODN, as therapeutic options for established mouse tumors. Immunization with control plasmid DNA partially lowered the tumor burden caused by the more aggressive B16-F10 variant of the B16 melanoma. Although mAb to TIM-3 alone afforded a small delay in tumor growth, it eventually failed to protect mice from developing tumors (**Fig. 3a**). In contrast, combined treatment with control plasmid DNA and mAb to TIM-3 resulted in substantial inhibition of tumor growth (**Fig. 3a** and data not shown). These results suggested that TIM-3 exerted a marginal effect because the release of endogenous DNA in untreated tumors was limited, but exogenous DNA administered therapeutically triggered a strong antitumor effect after blockade of TIM-3. Blockade of TIM-3 delayed tumor growth to a similar extent in combination with either control plasmid with no insert or TRP-2-encoding plasmid (data not shown), which suggested that TIM-3 regulated innate immune responses independently of a particular tumor antigen. Consistent with that, blockade of TIM-3 induced the antitumor activity of the plasmid encoding TRP-2 but not of a vaccine consisting of TRP-2 peptide (**Fig. 3a** and data not shown). Tumors from mice treated with both plasmid DNA and mAb to TIM-3

© 2012 Nature America, Inc. All rights reserved.

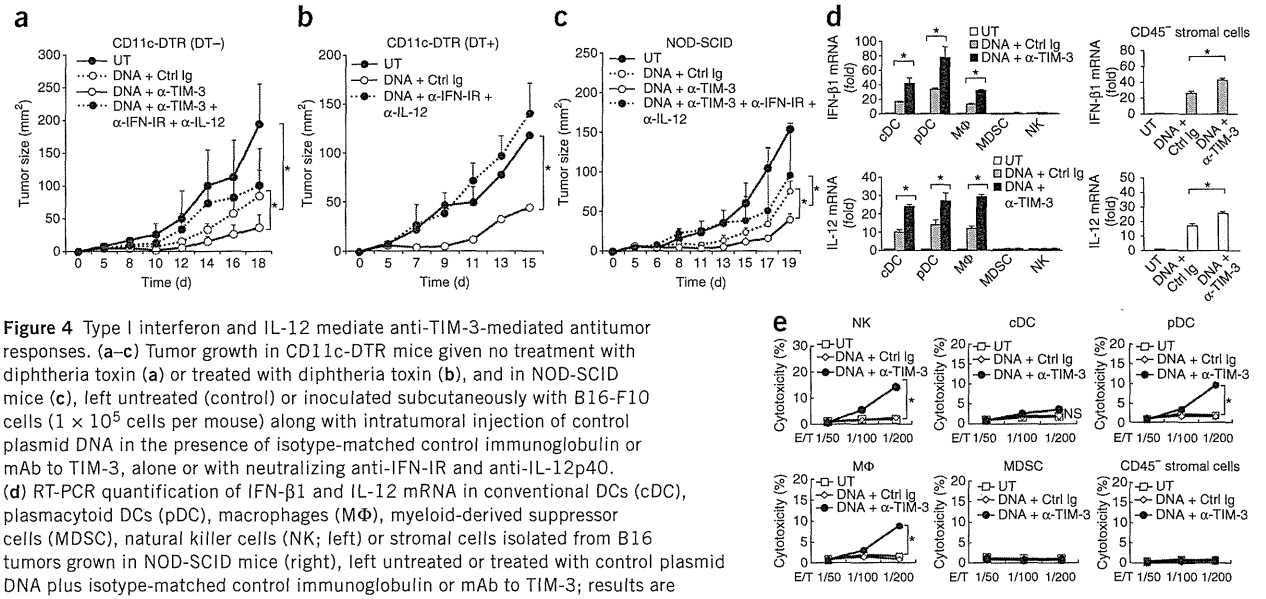

Figure 4 Type I interferon and IL-12 mediate anti-TIM-3-mediated antitumor responses. (**a–c**) Tumor growth in CD11c-DTR mice given no treatment with diphtheria toxin (**a**) or treated with diphtheria toxin (**b**), and in NOD-SCID mice (**c**), left untreated (control) or inoculated subcutaneously with B16-F10 cells (1×10^5 cells per mouse) along with intratumoral injection of control plasmid DNA in the presence of isotype-matched control immunoglobulin or mAb to TIM-3, alone or with neutralizing anti-IFN-IR and anti-IL-12p40. (**d**) RT-PCR quantification of IFN-β1 and IL-12 mRNA in conventional DCs (cDC), plasmacytoid DCs (pDC), macrophages (MΦ), myeloid-derived suppressor cells (MDSC), natural killer cells (NK; left) or stromal cells isolated from B16 tumors grown in NOD-SCID mice (right), left untreated or treated with control plasmid DNA plus isotype-matched control immunoglobulin or mAb to TIM-3; results are presented relative to *Actb* expression. (**e**) Cytotoxicity of the cells in **d** (effector cells; E) cultured together for 6 h with B16 cells (target cells; T) at various ratios (E/T), assessed by lactate dehydrogenase–release assay. $^*P < 0.05$ (paired Student's *t*-test). Data are representative of three experiments (**a**,**c–e**) or four experiments (**b**; error bars, s.e.m.).

had more IFN-β and IL-12 protein than did those from mice treated with mAb to TIM-3 or DNA alone (**Fig. 3b**), which indicated the close relationship between cytokine concentrations and antitumor effects.

To further define the role of DC-derived TIM-3 in circumventing the therapeutic efficacy of DNA vaccines, we treated B16-F10 melanomas with plasmid DNA and mAb to TIM-3 in CD11c-DTR mice, in which conditional depletion of CD11c$^+$ DCs can be achieved by administration of diphtheria toxin. In CD1c-DTR mice not treated with diphtheria toxin that had endogenous TIM-3^{hi} TADCs, control plasmid DNA plus mAb to TIM-3 protected mice from growing tumors more than control plasmid DNA alone did (**Fig. 3c**). In contrast, depletion of DCs from CD11c-DTR mice resulted in much greater antitumor effects of DNA alone in this model (**Fig. 3c**). To elucidate whether TIM-3 on DCs impeded antitumor responses mediated by nucleic acids, we adoptively transferred wild-type or TIM-3-deficient BMDCs into DC-deficient CD11c-DTR mice with B16-F10 melanoma. Treatment with control plasmid DNA was ineffective against established B16-F10 tumors in the presence of wild-type DCs, whereas treatment with control plasmid DNA induced profound inhibition of tumor growth after transfer of TIM-3-deficient DCs (**Fig. 3d**).

To further define the role of TIM-3 expressed on endogenous DCs in the antitumor effect of DNA adjuvant, we generated mixed–bone marrow chimeras that could be selectively depleted of TIM-3-expressing DCs from CD11c-DTR mice. We mixed bone marrow cells from TIM-3-deficient mice and CD11c-DTR mice at a ratio of 1:1 and used that mixture to reconstitute irradiated wild-type recipient mice, then compared the antitumor effects of control plasmid DNA in those chimeras treated with diphtheria toxin or not. Treatment with DNA alone restrained tumor growth more potently in diphtheria toxin–treated chimeras than in those not treated with diphtheria toxin, whereas mAb to TIM-3 had an inhibitory effect on tumor growth regardless of treatment with diphtheria toxin (**Fig. 3e**). Together these findings further exemplified the role of DC-specific TIM-3 in negatively regulating nucleic acid–mediated antitumor immunity. We observed similar synergistic antitumor effects of DNA and mAb to TIM-3 in mice of the nonobese diabetic–severe combined immunodeficiency (NOD-SCID) strain and C57BL/6 mice treated with depleting antibody to CD8 (anti-CD8) or control immunoglobulin (**Supplementary Fig. 4**). These results further confirmed that TIM-3 on CD8$^+$ T cells was not responsible for the synergistic activities of DNA and mAb to TIM-3, which differed from published observations suggesting that CD8$^+$ T cells are necessary for the exertion of antitumor responses induced by mAb to TIM-3 alone[21].

To determine the mechanisms by which the blockade of TIM-3 elicited antitumor responses, we focused on the contributions of type I interferon and IL-12 to the nucleic acid–triggered responses, because these are well-known antitumor effector cytokines. Indeed, the antitumor effect of control plasmid DNA was mostly abolished in diphtheria toxin–treated CD11c-DTR mice when the control plasmid DNA was administered together with neutralizing mAb to the receptor for type I interferon (IFN-IR) and mAb to IL-12. Moreover, the antitumor effect of mAb to TIM-3 and control plasmid DNA was also abrogated by the combined blockade of IFN-IR and IL-12 in CD11c-DTR mice not treated with diphtheria toxin or in NOD-SCID mice (**Fig. 4a–c**). Treatment with neutralizing antibody to IFN-IR, to IL-12 or to both had little effect on the growth of B16-F10 tumors in the absence of the administration of control plasmid DNA (data not shown), which indicated that immunogenic DNA was required for the triggering of antitumor responses by IFN-IR and IL-12.

CD11c^{lo}B220$^+$PDCA1$^+$ plasmacytoid DCs, CD11c^{hi} conventional DCs, F4/80$^+$CD11b$^+$ macrophages and CD45$^-$gp38$^+$ stromal cells were the main producers of type I interferon and IL-12 in the tumor microenvironments of NOD-SCID mice after treatment with control plasmid DNA and mAb to TIM-3 (**Fig. 4d**). Moreover, cytotoxic activity was much greater in natural killer cells, macrophages and plasmacytoid DCs of NOD-SCID mice treated with control plasmid DNA and mAb to TIM-3 than in those of mice treated with control plasmid DNA alone (**Fig. 4e**), consistent with published reports that the appropriate innate immune adjuvants may trigger the antitumor effector functions of plasmacytoid DCs[22]. In CD11c-DTR mice depleted of DCs, the main sources of IFN-β1 and IL-12 were

© 2012 Nature America, Inc. All rights reserved.

– 292 –

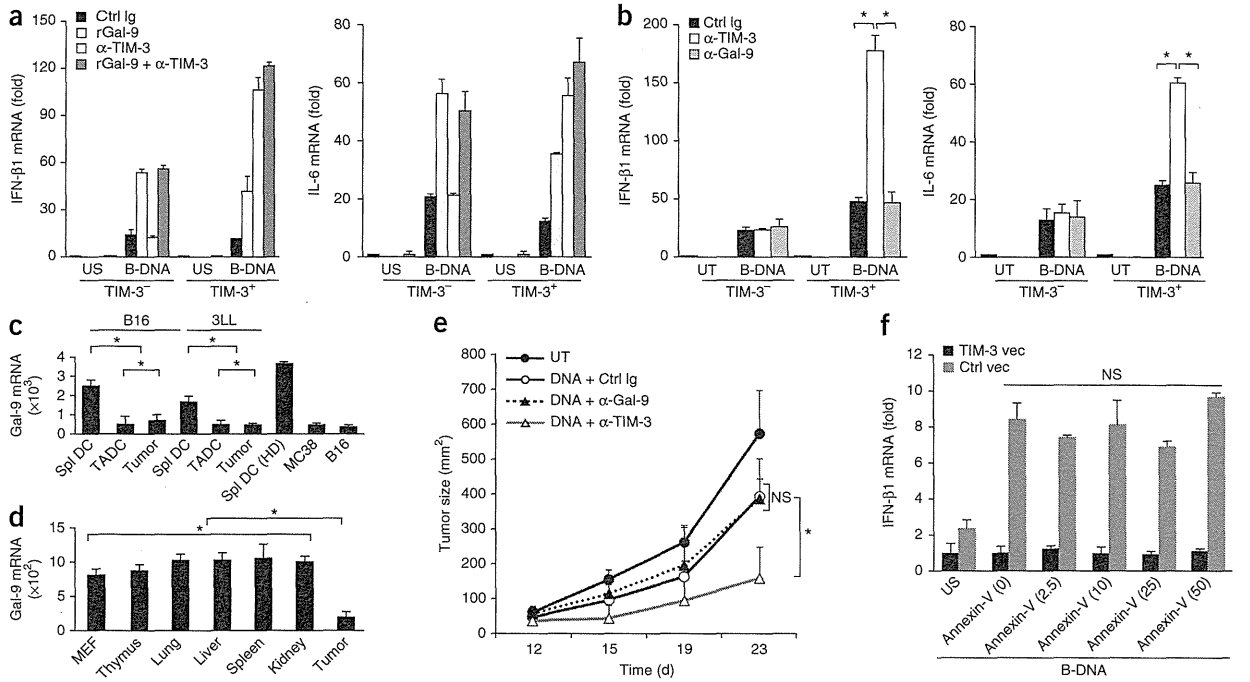

Figure 5 TIM-3 regulates innate responses by a galectin-9-independent mechanism. (**a**) RT-PCR analysis of IFN-β1 and IL-6 mRNA in wild-type TIM-3$^+$ and TIM-3$^-$ BMDCs pretreated with isotype-matched control immunoglobulin, recombinant galectin-9 (rGal-9) and/or mAb to TIM-3 (key), followed by no stimulation or stimulation for 8 h with B-DNA; results are presented relative to *Actb* expression. (**b**) RT-PCR quantification of IFN-β1 and IL-6 mRNA in TIM-3$^+$ and TIM-3$^-$ BMDCs left untreated or treated for 24 h with B-DNA in the presence of isotype-matched control immunoglobulin, mAb to TIM-3 or mAb to galectin-9; results are presented relative to *Actb* expression. (**c**) RT-PCR quantification of galectin-9 (Gal-9) mRNA in splenic DCs (Spl DC), TADCs and tumor cells isolated from established B16 or 3LL tumors, splenic DCs from non-tumor-bearing mice (HD) and MC38 or 3LL tumor cells cultured *in vitro*; results are presented relative to *Actb* expression. (**d**) RT-PCR quantification of galectin-9 mRNA in MEFs, normal tissues (thymus, lung, liver, spleen and kidney) from tumor-bearing mice, and B16 tumors (Tumor); results are presented relative to expression of *Gapdh* (reference gene encoding glyceraldehyde phosphate dehydrogenase). (**e**) Tumor growth in C57BL/6 mice ($n = 4$ per group) left untreated or inoculated subcutaneously with B16-F10 melanoma cells (1×10^5 cells per mouse) and given intratumoral injection of control plasmid DNA in the presence of isotype-matched control immunoglobulin or mAb to galectin-9 or TIM-3. (**f**) RT-PCR analysis of IFN-β1 mRNA in MEFs transfected for 24 h with vector encoding TIM-3 or control vector, then left unstimulated or stimulated with B-DNA in the presence of various concentrations of recombinant annexin V (horizontal axis; in ng/ml). $^*P < 0.05$ (paired Student's *t*-test). Data are representative of three experiments (**a–e**) or two experiments (**f**; error bars, s.e.m.).

© 2012 Nature America, Inc. All rights reserved.

macrophages and CD45$^-$stromal cells, and natural killer cells and macrophages were main effectors involved in killing tumor cells in an IFN-IR- and IL-12-dependent manner (data not shown). Together these results suggested that blockade of TIM-3 might convert tolerogenic cells of the innate immune system into antitumor effector cells and that type I interferon and IL-12, as well as various innate cells, act as downstream effectors to trigger antitumor responses mediated by DNA and mAb to TIM-3.

TIM-3 regulates innate response independently of galectin-9

The interaction between galectin-9 and TIM-3 on myeloid cells elicits antimicrobial and antitumor immunity but inhibits T helper type 1 responses[23–25]. However, treatment with recombinant galectin-9 or mAb to galectin-9 did not suppress B-DNA-mediated cytokine production in TIM-3$^+$ or TIM-3$^-$ DCs (**Fig. 5a,b**). We detected much less galectin-9 mRNA in TADCs and tumor cells than in splenic DCs derived from tumor-bearing or normal mice (**Fig. 5c**). Bulk tumor tissues also had significantly less galectin-9 mRNA than did normal tissues in B16 tumor–bearing mice (**Fig. 5d**), which indicated that galectin-9 production was compromised in tumors. Furthermore, treatment with mAb to galectin-9 did not enhance the antitumor effects of control plasmid DNA (**Fig. 5e**).

In addition to galectin-9, phosphatidylserine exposed by apoptotic cells is a TIM-3 ligand[26,27]. However, treatment with annexin V, which also binds phosphatidylserine and potentially competes with TIM-3, had little effect on B-DNA-mediated expression of the gene encoding IFN-β1 in TIM-3$^+$ MEFs (**Fig. 5f**), which suggested that TIM-3-mediated regulation of nucleic acid sensing was independent of the recognition of phosphatidylserine on apoptotic cells. Together these findings demonstrated that DC-derived TIM-3 recognized a ligand other than galectin-9 or phosphatidylserine to suppress nucleic acid–mediated immune responses.

TIM-3 serves as a receptor for HMGB1

In HEK293 cells, B-DNA is recognized by the intracellular receptor RIG-I through the induction of an RNA polymerase III–transcribed RNA intermediate[28]. TIM-3 had little inhibitory effect on the IFN-β1 response in HEK293 cells transfected with expression vectors for RIG-I or the signaling adapters STING, MAVS, MyD88 and TRIF (data not shown). This indicated that TIM-3 acted on nucleic acid–sensing systems upstream of PRR-specific pathways.

HMGB1 is an evolutionarily conserved nuclear protein that acts on various cells and interacts with many different types of ligands, such as RAGE, TLR4 and so on, to modulate pleiotropic functions of

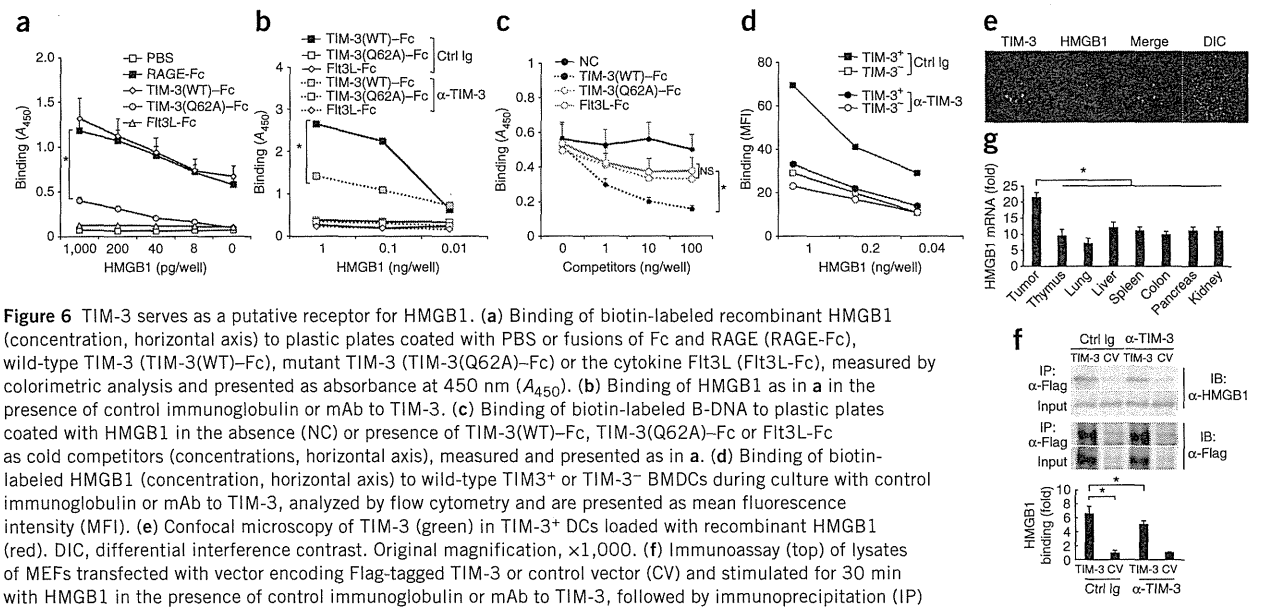

Figure 6 TIM-3 serves as a putative receptor for HMGB1. (**a**) Binding of biotin-labeled recombinant HMGB1 (concentration, horizontal axis) to plastic plates coated with PBS or fusions of Fc and RAGE (RAGE-Fc), wild-type TIM-3 (TIM-3(WT)–Fc), mutant TIM-3 (TIM-3(Q62A)–Fc) or the cytokine Flt3L (Flt3L-Fc), measured by colorimetric analysis and presented as absorbance at 450 nm (A_{450}). (**b**) Binding of HMGB1 as in **a** in the presence of control immunoglobulin or mAb to TIM-3. (**c**) Binding of biotin-labeled B-DNA to plastic plates coated with HMGB1 in the absence (NC) or presence of TIM-3(WT)–Fc, TIM-3(Q62A)–Fc or Flt3L-Fc as cold competitors (concentrations, horizontal axis), measured and presented as in **a**. (**d**) Binding of biotin-labeled HMGB1 (concentration, horizontal axis) to wild-type TIM3$^+$ or TIM-3$^-$ BMDCs during culture with control immunoglobulin or mAb to TIM-3, analyzed by flow cytometry and are presented as mean fluorescence intensity (MFI). (**e**) Confocal microscopy of TIM-3 (green) in TIM-3$^+$ DCs loaded with recombinant HMGB1 (red). DIC, differential interference contrast. Original magnification, ×1,000. (**f**) Immunoassay (top) of lysates of MEFs transfected with vector encoding Flag-tagged TIM-3 or control vector (CV) and stimulated for 30 min with HMGB1 in the presence of control immunoglobulin or mAb to TIM-3, followed by immunoprecipitation (IP) with mAb M2 to the Flag tag and immunoblot analysis with anti-HMGB1 or anti-Flag. Bottom, band intensity of HMGB1–TIM-3 in MEFs transfected with TIM-3 relative to that in MEFs transfected with control vector (below). (**g**) RT-PCR quantification of HMGB1 mRNA in B16-F10 tumors and normal tissues; results are presented relative to *Actb* expression. $^*P < 0.05$ (paired Student's *t*-test). Data are representative of five experiments (**a**,**f**), four experiments (**b**,**c**) or three experiments (**d**,**e**,**g**; error bars (**a**,**c**,**d**,**f**,**g**), s.e.m.).

these entities in various physiological and pathological situations[29]. HMGB1 also has an essential role in activating innate immune responses mediated by sensors of nucleic acids[30,31]; therefore, we investigated potential interactions between HMGB1 and TIM-3. We indeed found that TIM-3 bound HMGB1 with an affinity similar to that of RAGE, a known receptor for HMGB1 (**Fig. 6a**). Furthermore, the interaction between HMGB1 and TIM-3 was partially suppressed in the presence of a fusion of RAGE and the Fc portion of immunoglobulin or galectin-9 protein (**Supplementary Fig. 5a**), which confirmed the specificity of the interaction between HMGB1 and TIM-3 in this analysis.

TIM-3 binds phosphatidylserine through a metal ion–dependent ligand-binding site in its FG loop[32,33]. We therefore constructed a fusion of mutant TIM-3 and the Fc portion of immunoglobulin, with the glutamine at position 62 near the FG loop of TIM-3 (at the galectin-9-independent ligand-binding site) replaced with alanine (Tim-3(Q62A)–Fc)[32]. This substitution largely abrogated the ability of TIM-3 to bind HMGB1 (**Fig. 6a**), which indicated that the metal ion–dependent ligand-binding portion of TIM-3 was critical for binding HMGB1. In addition, the interaction of a fusion of wild-type TIM-3 and Fc (TIM-3(WT)–Fc) with HMGB1 was blocked by mAb to TIM-3 (**Fig. 6b**).

HMGB1 has DNA-binding domains in its A-box and B-box, and its interaction with DNA is enhanced by the tail domain at its carboxyl terminus[29]. Thus, we determined whether TIM-3 and nucleic acids competed for binding to the same domain of HMGB1. Indeed, the binding of either B-DNA or TIM-3 (WT)–Fc to HMGB1 was mostly abrogated by deletion of the A-box but not by deletion of the B-box or carboxy-terminal domain (**Supplementary Fig. 5b,c**). Furthermore, the binding of biotin-labeled B-DNA to HMGB1 was inhibited by unlabeled TIM-3 (WT)–Fc in a concentration-dependent manner. In contrast, unlabeled TIM-3(Q62A)–Fc did not inhibit the interaction between B-DNA and HMGB1 (**Fig. 6c**), which indicated that TIM-3 and nucleic acids competed with each other for binding to A-box domain of HMGB1.

Moreover, wild-type TIM-3$^+$ DCs interacted with biotin-labeled HMGB1 with a higher affinity than that of wild-type TIM-3$^-$ DCs, although both were inhibited by mAb to TIM-3 (**Fig. 6d**). There was detectable binding of HMGB1 to TIM-3$^-$ DCs, although it was much lower than the binding of HMGB1 to their TIM-3$^+$ counterparts (**Fig. 6d**), which suggested that some other receptors, such as RAGE, may have been involved in the binding of HMGB1 to TIM-3$^-$ DCs. TIM-3 was also located together with HMGB1 in TIM-3$^+$ DCs (**Fig. 6e**) and bound to HMGB1 in MEFs transfected to express TIM-3. Furthermore, densitometry of immunoprecipitated bands showed that the inhibitory effect of mAb to TIM-3 on this binding was significant (**Fig. 6f**). Tumors had significantly more HMGB1 mRNA than did normal tissues (**Fig. 6g**), which indicated that in contrast to galectin-9 production, HMGB1 production occurred in tumors. Together these results identified TIM-3 as a putative receptor for HMGB1 in DCs in tumor microenvironments.

TIM-3 inhibits the recruitment of nucleic acids into endosomes

Proper trafficking of nucleic acids into endosomal vesicles is a key event in the initiation of innate immune signaling. Danger-associated molecules such as uric acid and HMGB proteins form complexes with nucleic acids and allow them access to endosomal vesicles and allow the triggering of immune responses[34]. We therefore investigated whether HMGB1 directly affected the recruitment of nucleic acids into endosomal vesicles. For this, we adopted an experimental system of HMGB1-deficient MEFs 'loaded' with recombinant HMGB1 proteins. Consistent with the role of HMGB1 in mediating the sensing of nucleic acids by the immune system, the addition of HMGB1 facilitated more transfer of B-DNA into endosomal vesicles positive for the early endosomal marker EEA1 in HMGB1-deficient MEFs than in HMGB1-competent wild-type cells (**Fig. 7a**). In contrast, B-DNA was located mainly around the plasma membrane, but the recruitment of B-DNA into endosomal vesicles was much lower in HMGB1-deficient MEFs transfected to express TIM-3 tagged with

© 2012 Nature America, Inc. All rights reserved.

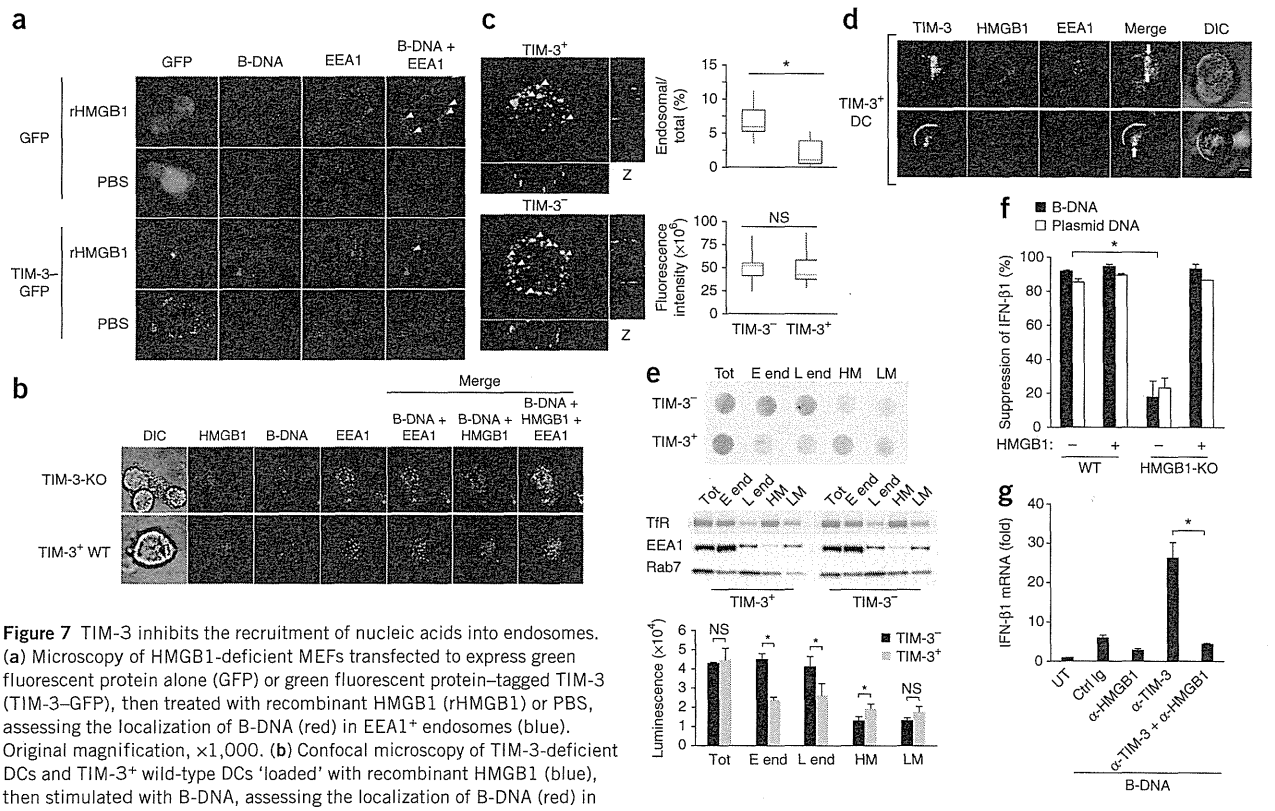

Figure 7 TIM-3 inhibits the recruitment of nucleic acids into endosomes. (**a**) Microscopy of HMGB1-deficient MEFs transfected to express green fluorescent protein alone (GFP) or green fluorescent protein–tagged TIM-3 (TIM-3–GFP), then treated with recombinant HMGB1 (rHMGB1) or PBS, assessing the localization of B-DNA (red) in EEA1$^+$ endosomes (blue). Original magnification, ×1,000. (**b**) Confocal microscopy of TIM-3-deficient DCs and TIM-3$^+$ wild-type DCs 'loaded' with recombinant HMGB1 (blue), then stimulated with B-DNA, assessing the localization of B-DNA (red) in EEA1$^+$ endosomes (green). Original magnification, ×1,000. (**c**) Quantification of the fluorescence intensity of total cellular B-DNA (red (left); bottom right) and B-DNA in EEA1$^+$ endosomes (green (left)) relative to total cellular B-DNA (top right) in wild-type TIM-3$^+$ or TIM-3$^-$ BMDCs in images (left) acquired from the bottom to the top of the cells in **b**. Original magnification, ×1,200. (**d**) Confocal microscopy of the localization of TIM-3 (green) and HMGB1 (blue) in EEA1$^+$ endosomes (red) in TIM-3$^+$ DCs. Original magnification, ×1,000. (**e**) Dot-blot analysis of B-DNA (top) and immunoblot analysis of transferrin receptor (TfR), EEA1 and the late endosome marker Rab7 (middle) in total lysates (Tot), early endosomes (E end), late endosomes (L end) and heavy (HM) or light (LM) plasma membrane fractions isolated from homogenized BMDCs 2 h after treatment with B-DNA. Bottom, quantification of the dot-blot results above. (**f**) Suppression of IFN-β1 in wild-type or HMGB1-deficient (HMGB1-KO) MEFs transfected to express TIM-3, followed by stimulation with B-DNA or control plasmid DNA with (+) or without (–) recombinant HMGB1; results are presented relative to those of cells transfected with control vector. (**g**) RT-PCR analysis of IFN-β1 mRNA in TIM-3$^+$ BMDCs left untreated or pretreated with isotype-matched control immunoglobulin or anti-HMGB1 and/or mAb to TIM-3 (horizontal axis), followed by stimulation for 8 h with B-DNA; results are presented relative to *Actb* expression. *$P < 0.05$ (paired Student's *t*-test). Data are representative of four experiments (**a**), three experiments (**b**,**e**–**g**) or five experiments (**d**) or are pooled from three separate experiments with 30 cells (**c**; error bars (**c**,**e**–**g**), s.e.m.).

© 2012 Nature America, Inc. All rights reserved.

green fluorescent protein, followed by stimulation with HMGB1, than in wild-type MEFs (**Fig. 7a**), which suggested that TIM-3 interfered with HMGB1-dependent transfer of nucleic acids to the endosome. To further investigate whether endogenous TIM-3 had an inhibitory effect on the recruitment of nucleic acids to the endosome, we evaluated the endosomal localization of nucleic acids such as B-DNA or CpG-ODN in wild-type TIM-3$^+$ DCs or TIM-3-deficient TIM-3$^-$ DCs. A much greater portion of nucleic acids was localized to endosomal vesicles in TIM-3-deficient DCs than in wild-type TIM-3$^+$ DCs after stimulation with nucleic acids and HMGB1 (**Fig. 7b** and data not shown).

We next quantified B-DNA in total and EEA1$^+$ early endosomal vesicles in wild-type TIM-3$^+$ and TIM-3$^-$ DCs through the use of image-processing software[35]. The EEA1$^+$ endosomal vesicles of TIM-3$^+$ DCs had less B-DNA than did those of TIM-3$^-$ DCs, whereas total B-DNA was similar in both populations (**Fig. 7c**). Consistent with those findings, TIM-3 mainly localized together with HMGB1 in EEA1$^+$ endosomal vesicles in TIM-3$^+$ DCs after stimulation with HMGB1 (**Fig. 7d**).

To further substantiate the differences in the recruitment of DNA into endosomal vesicles in TIM-3$^+$ and TIM-3$^-$ cells, we purified endosomal vesicles by subcellular fractionation to measure the recruitment of DNA in wild-type TIM-3$^+$ or TIM-3$^-$ DCs. We confirmed that TIM-3$^+$ and TIM-3$^-$ DCs had similarly expression of the markers for early endosomes and late endosomes, as well as transferrin receptor (**Fig. 7e**). As expected, dot-blot analysis showed much less B-DNA in purified early or late endosomal vesicles from TIM-3$^+$ DCs than in those from TIM-3$^-$ DCs, whereas we detected more B-DNA in the heavy membrane fractions of TIM-3$^+$ DCs than in their TIM-3$^-$ counterparts. There was little difference between TIM-3$^+$ DCs and TIM-3$^-$ DCs in the amount of endocytosed DNA in the total and light plasma membrane fractions (**Fig. 7e**). Moreover, endosomal vesicles purified from HMGB1-stimulated TIM-3$^+$ DCs had less uptake of B-DNA than did those of HMGB1-stimulated TIM-3$^-$ DCs, as quantified by flow cytometry (**Supplementary Fig. 6**). Together these results demonstrated a role for TIM-3 in restraining the transport of nucleic acids to endosome, which is normally triggered by HMGB1.